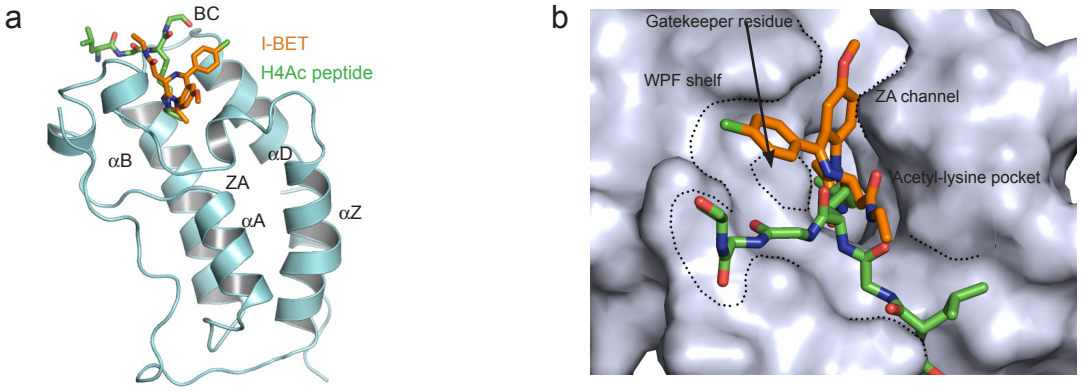

c

```
                                  |~~~ ~~~~αZ~~~~~~|                  ZA loop                 |~~αA
BRD2_BD1     61  PPPPEVSNPK KPGRVTNQLQ YLHKVVMKAL WK---HQFAW PFRQPVDAVK LGLPDYHKII KQPMDMGTIK
BRD3_BD1     21  PPPPEVSNPS KPGRKTNQLQ YMQNVVVKTL WK---HQFAW PFYQPVDAIK LNLPDYHKII KNPMDMGTIK
BRD4_BD1     45  PPPPETSNPN KPKRQTNQLQ YLLRVVLKTL WK---HQFAW PFQQPVDAVK LNLPDYYKII KTPMDMGTIK
BRD2_BD2    339  --------QS SKKGKLSEQL KHCNGILKEL LSKKHAAYAW PFYKPVDASA LGLHDYHDII KHPMDLSTVK
BRD3_BD2    301  --------HA GKKGKLSEHL RYCDSILREM LSKKHAAYAW PFYKPVDAEA LELHDYHDII KHPMDLSTVK
BRD4_BD2    343  --------AP EKSSKVSEQL KCCSGILKEM FAKKHAAYAW PFYKPVDVEA LGLHDYCDII KHPMDMSTIK

             αA~~|       |~~~~~~~~αB ~~~~~~| BC loop  |~~ ~~~~~~αC~~ ~~~~~|
BRD2_BD1    128  RRLENNYYWA ASECMQDFNT MFTNCYIYNK P----TDDIV LMAQTLEKIF LQKVASMPQE
BRD3_BD1     88  KRLENNYYWS ASECMQDFNT MFTNCYIYNK P----TDDIV LMAQALEKIF LQKVAQMPQE
BRD4_BD1    112  KRLENNYYWN AQECIQDFNT MFTNCYIYNK P----GDDIV LMAEALEKLF LQKINELPTE
BRD2_BD2    401  RKMENRDYRD AQEFAADVRL MFSNCYKYNP P----DHDVV AMARKLQDVF EFRYAKMPDE
BRD3_BD2    363  RKMDGREYPD AQGFAADVRL MFSNCYKYNP P----DHEVV AMARKLQDVF EMRFAKMPDE
BRD4_BD2    405  SKLEAREYRD AQEFGADVRL MFSNCYKYNP P----DHEVV AMARKLQDVF EMRFAKMPDE
```

d

Protein construct	Compound	Temperature (°C)	K_D (nM)	DH (kcal/mol)	DS (cal/mol)	N (protein:ligand)
BRD2	I-BET	25	61.3	-28.2	-28.2	0.54:1
BRD3	I-BET	25	50.5	-22.4	-22.4	0.47:1
BRD4	I-BET	25	55.2	-30.5	-30.5	0.48:1
BRD4	inactive I-BET	25	-	-	-	-

e

Protein	K_D (ITC)	IC_{50} (FRET)
BRD2	61.3 nM (± 11.6 nM)	32.5 nM (± 6.3 nM)
BRD3	50.5 nM (± 9.9 nM)	42.4 nM (± 3.8 nM)
BRD4	55.2 nM (± 11.4 nM)	36.1 nM (± 2.5 nM)

f

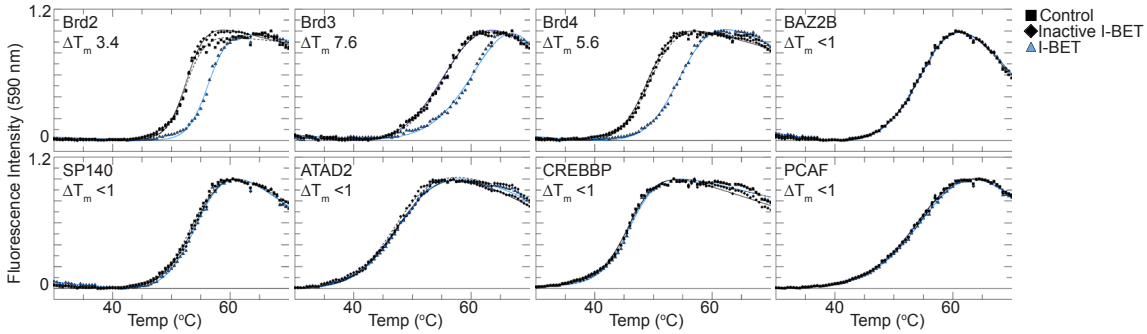

Supplementary Figure 1. Characterization of I-BET binding to BET proteins.
a, Ribbon representation of BRD4-BD1 bound to I-BET (orange) overlaid with H4(1-15)K12Ac peptide (green). Structural elements of BRD4-BD1 are labelled. **b,** BRD4-BD1 structure with key recognition and specificity pockets for I-BET binding indicated. **c,** Conservation of I-BET binding residues in BRD2, BRD3 and BRD4 bromodomains. Multiple sequence alignment of human *brd2*, *brd3* and *brd4* bromodomains 1 and 2 (BD1 and BD2) are shown. Highlighted in green are the 'gatekeeper residues' conserved in BD1 and BD2 of *brd2*, *brd3* and *brd4*. The WPF motif is highlighted in yellow, and the conserved tyrosine and asparagine that are key to acetylated lysine recognition are highlighted in blue. **d,** Summary table of isothermal titration calorimetry (ITC) experiments. DH is the enthalpy change on binding, DS is the entropy, N is the ratio of BET protein to I-BET. **e,** Summary Table of K_D of I-BET interaction with BRD2, BRD3 and BRD4 and IC_{50} values of I-BET mediated H4Ac peptide displacement from BRD2, BRD3 and BRD4 as obtained from ITC and FRET analysis respectively. **f,** Thermal shift assays of bromodomain-containing proteins in the presence of I-BET. His6-tagged BRD2 (1-473), BRD3 (1-434), BRD4 (1-477), BAZ2B (1858-1972), SP140 (687-867), ATAD2 (950-1148), CREBBP (1084-1197), PCAF (715-831) were subjected to temperature ramping (4-94°C) either alone (black squares) or in the presence of 20 μM of I-BET (blue triangles) or inactive I-BET (black diamonds), ΔTm is indicated. Lack of shift indicates lack of binding.

a

Table 1 Data collection and refinement statistics (**Molecular replacement**)

	BRD4-IBET
Data collection	
Space group	$P2_12_12_1$
Cell dimensions	
a, *b*, *c* (Å)	37.4, 44.3, 78.3
α, β, γ (°)	90.0, 90.0, 90.0
Resolution (Å)	78.3-1.6 (1.7-1.6) *
R_{merge}	0.114 (0.329)
$I/\sigma I$	10.9 (3.4)
Completeness (%)	95.4 (77.4)
Redundancy	6.1 (3.8)
Refinement	
Resolution (Å)	38.58-1.60
No. reflections	16, 134 (908)
R_{work}/ R_{free}	0.155/0.185
No. atoms	1388
Protein	1078
Ligand/ion	30/16
Water	264
B-factors	
Protein	16.2
Ligand/ion	13.2/40.1
Water	33.5
R.m.s deviations	
Bond lengths (Å)	0.007
Bond angles (º)	1.055

Number of crystals for each structure should be noted in footnote.
*Highest resolution shell is shown in parenthesis.

b

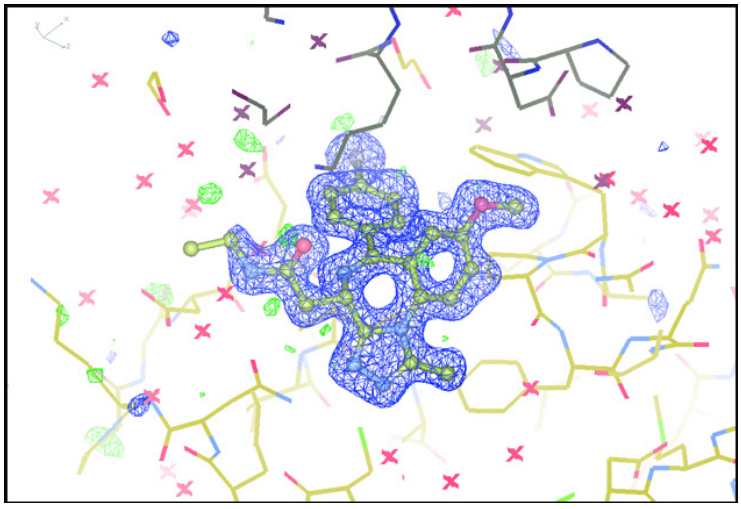

Supplementary Figure 2. Data collection and refinement statistics of X-ray analysis of the co-crystal structure of I-BET with BRD4-BD1. **a,** Table of X-ray refinement statistics. **b,** Difference electron map for I-BET after removal of the I-BET compound from the final X-ray structure model. The map is contoured at +/- 3 sigma, in blue and green respectively. The modeling of the binding mode of I-BET is unambiguous with all elements of the molecule clearly defined.

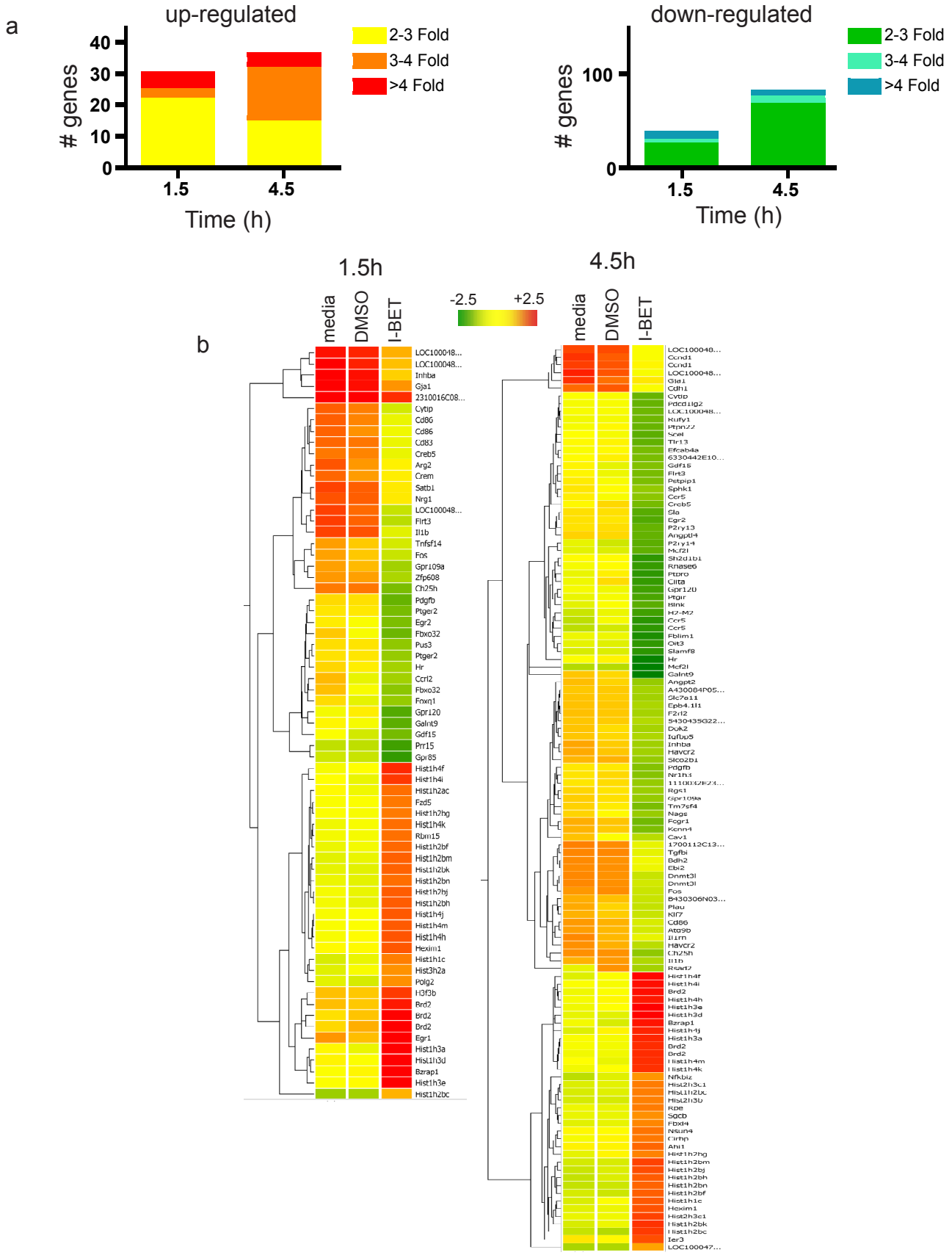

Supplementary Figure 3. Effect of I-BET on gene expression in resting macrophages. a, Bar diagrams show the number of up-regulated (left) or down-regulated (right) genes in BMDMs treated with I-BET alone, as compared to DMSO treated controls, for indicated time periods. Colours indicate the fold change of gene expression. **b,** Heatmap representation of all genes up- or down-regulated (>2-fold) by I-BET treatment as compared to medium or DMSO treated controls at 1.5 hours (left panel) and 4.5 hours (right panel).

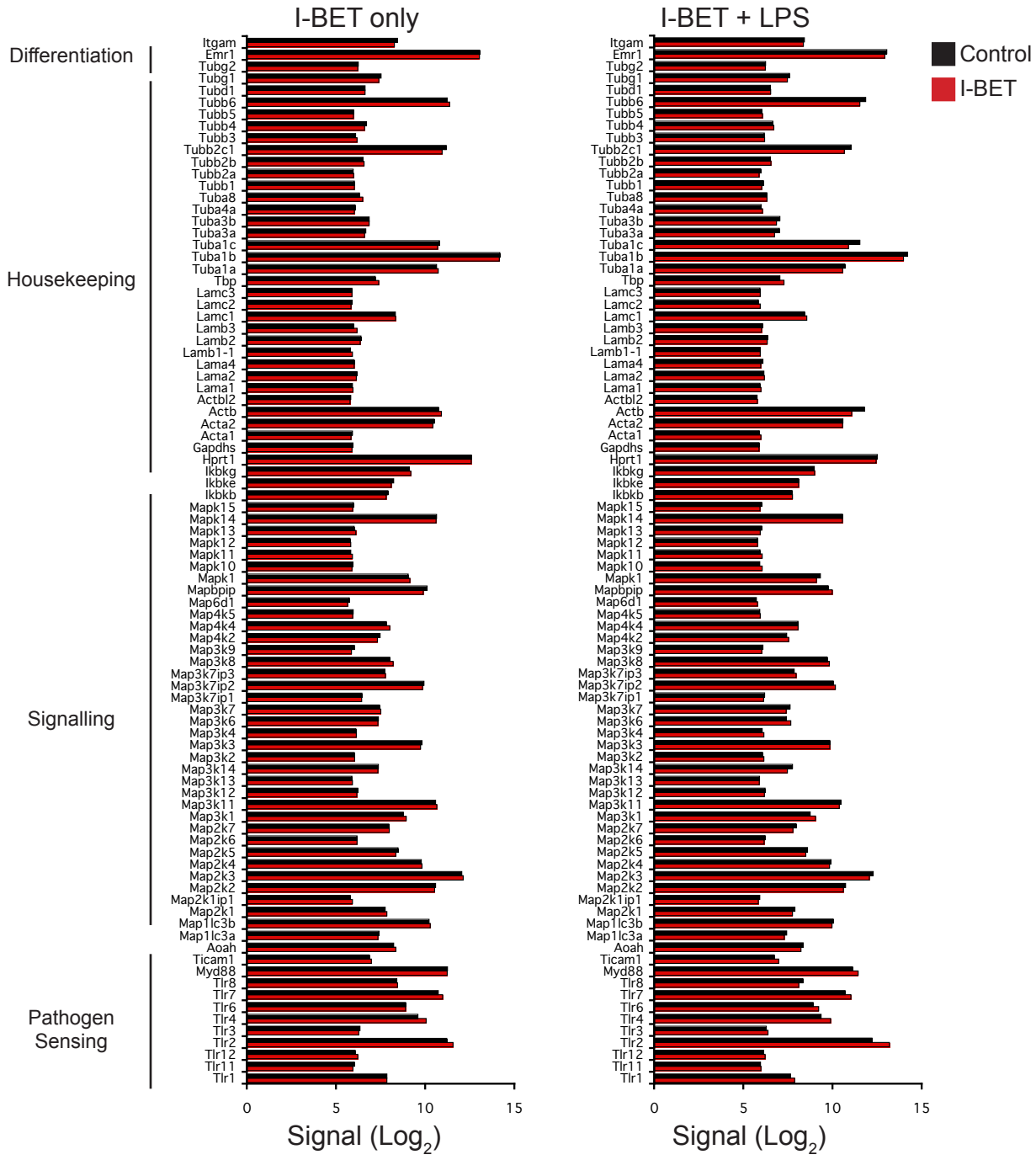

Supplementary Figure 4. I-BET does not alter expression of housekeeping, lineage-specific, pathogen sensing or signalling genes. Bar graphs show expression of macrophage differentiation markers, housekeeping genes, signalling and pathogen sensing genes in resting or LPS stimulated (1 hour) macrophages. Expression levels of genes in macrophages that were pre-treated with I-BET (red) or DMSO as a control (black) were determined by microarray (Illumina).

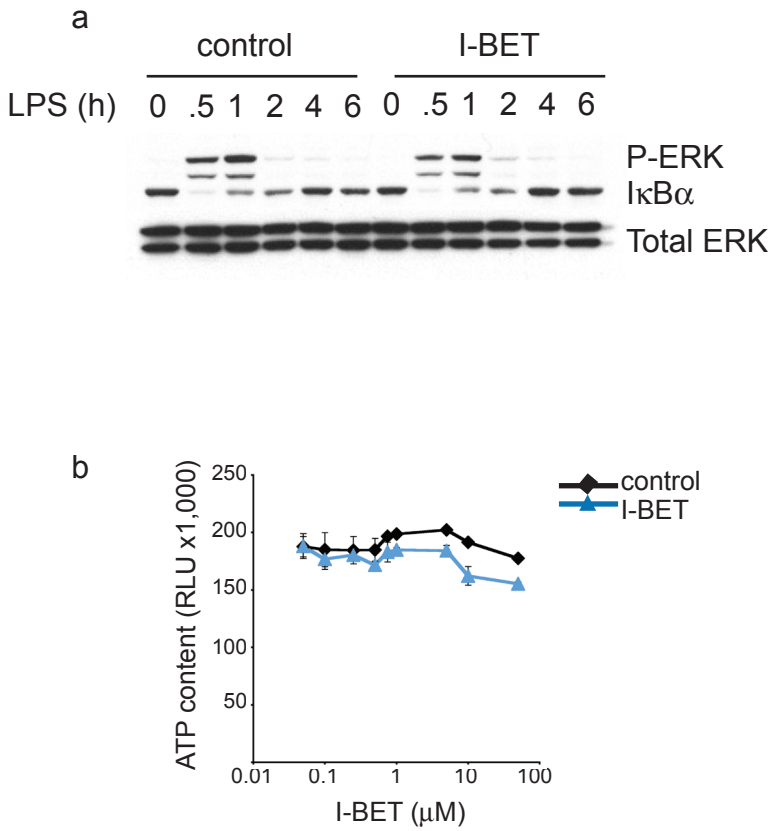

Supplementary Figure 5. LPS-induced signalling and survival are unaffected by I-BET. a, Signalling downstream of Toll-like receptor 4 (TLR4) in DMSO (control) or I-BET treated (I-BET) macrophages was evaluated by analysis of the kinetics and amplitude of LPS-induced ERK phosphorylation and IκB degradation. Data are representative of 3 independent experiments. **b,** I-BET has no impact on survival of macrophages. Viability of macrophages was determined by measurement of cellular ATP content (Cell-Titer Glo, Promega) after 4 hours of incubation with I-BET (blue triangles) or DMSO as a control (black diamonds) at indicated concentrations. Data are representative of 2 independent experiments performed in triplicate, error bars are s.d. of the triplicate.

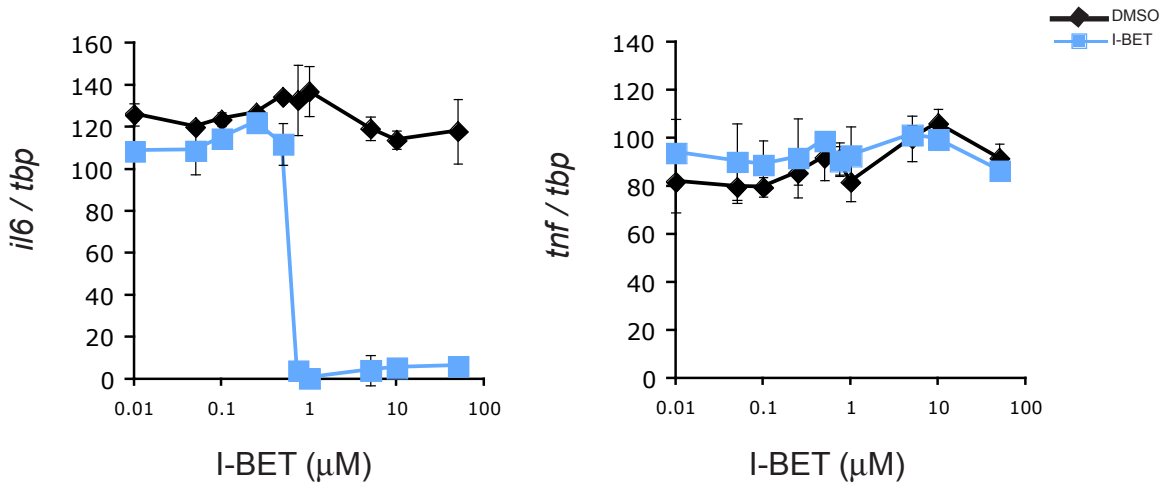

Supplementary Figure 6. *tnf* is resistant to I-BET at high doses. BMDMs were pre-treated with increasing amounts of I-BET (blue squares) or DMSO as a control (black diamonds) for 30 minutes before LPS stimulation (100 ng/mL) for 4 hours. Expression levels of *il6* and *tnf* genes were determined by qPCR analysis. Data are the mean of 3 independent experiments. Error bars represent the s.e.m.

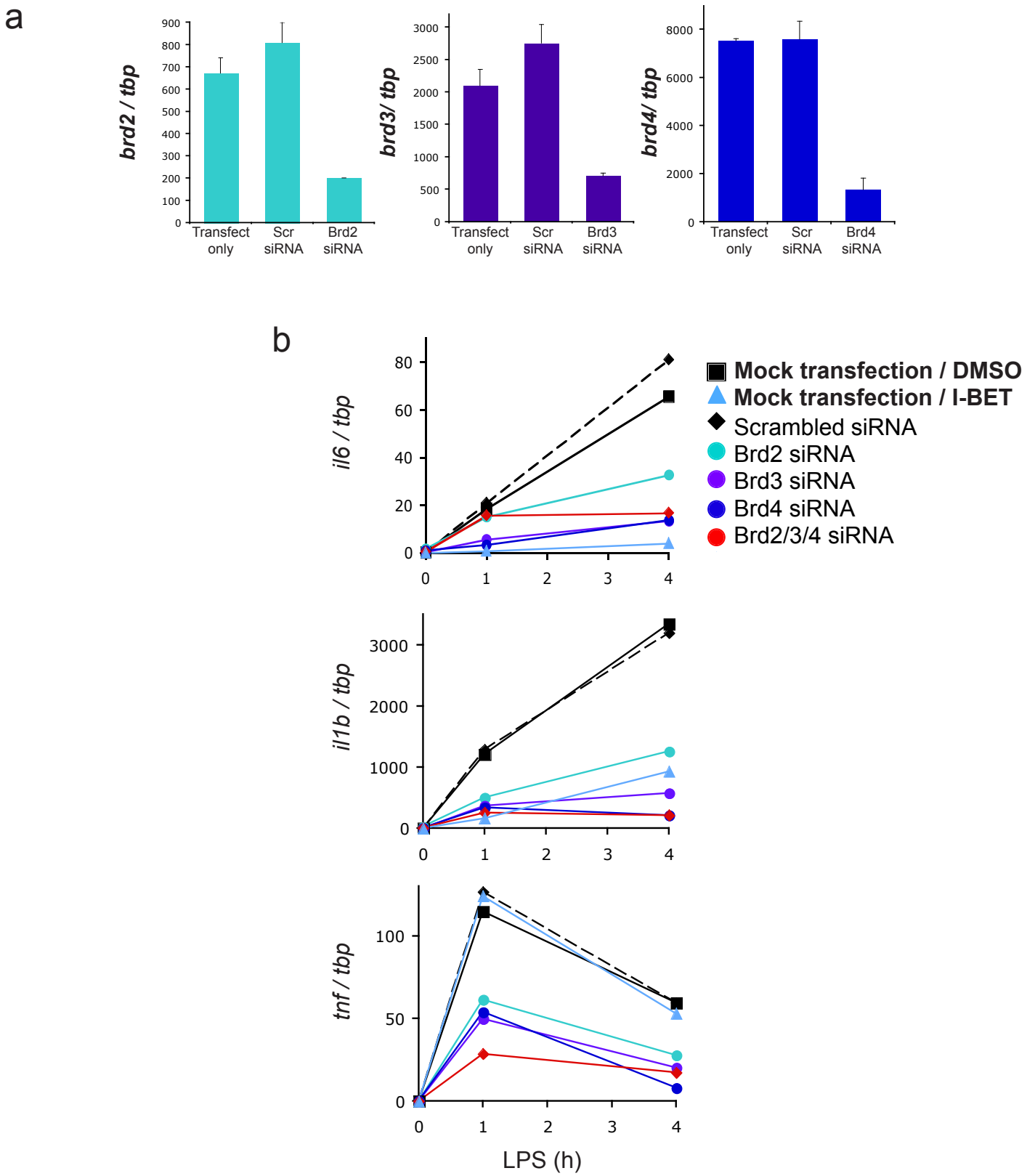

Supplementary Figure 7. RNAi knockdown of BET genes suppresses cytokine production in LPS-stimulated macrophages. a, RNAi knockdown of BET genes. BMDMs were mock-transfected or transfected with siRNA oligonucleotides against *brd2*, *brd3*, *brd4* or a scrambled siRNA (scr) control. *brd2*, *brd3* and *brd4* mRNA expression levels were measured by qPCR at 48 hours after transfection. Data are representative of two independent experiments performed in triplicate. Error bars are s.d. of the triplicate. **b,** Following siRNA mediated BET gene knockdown (single or a combination of all 3), that was confirmed by qPCR, macrophages were treated with LPS for indicated times. To compare the effect of I-BET treatment to BET knockdown, mock-transfected cells were either pre-treated with DMSO as a control (black squares) or 1 M of I-BET (blue triangles) for 30 minutes before LPS stimulation. *il6, il1b* and *tnf* mRNA levels were determined by qPCR. Data are representative of two independent experiments.

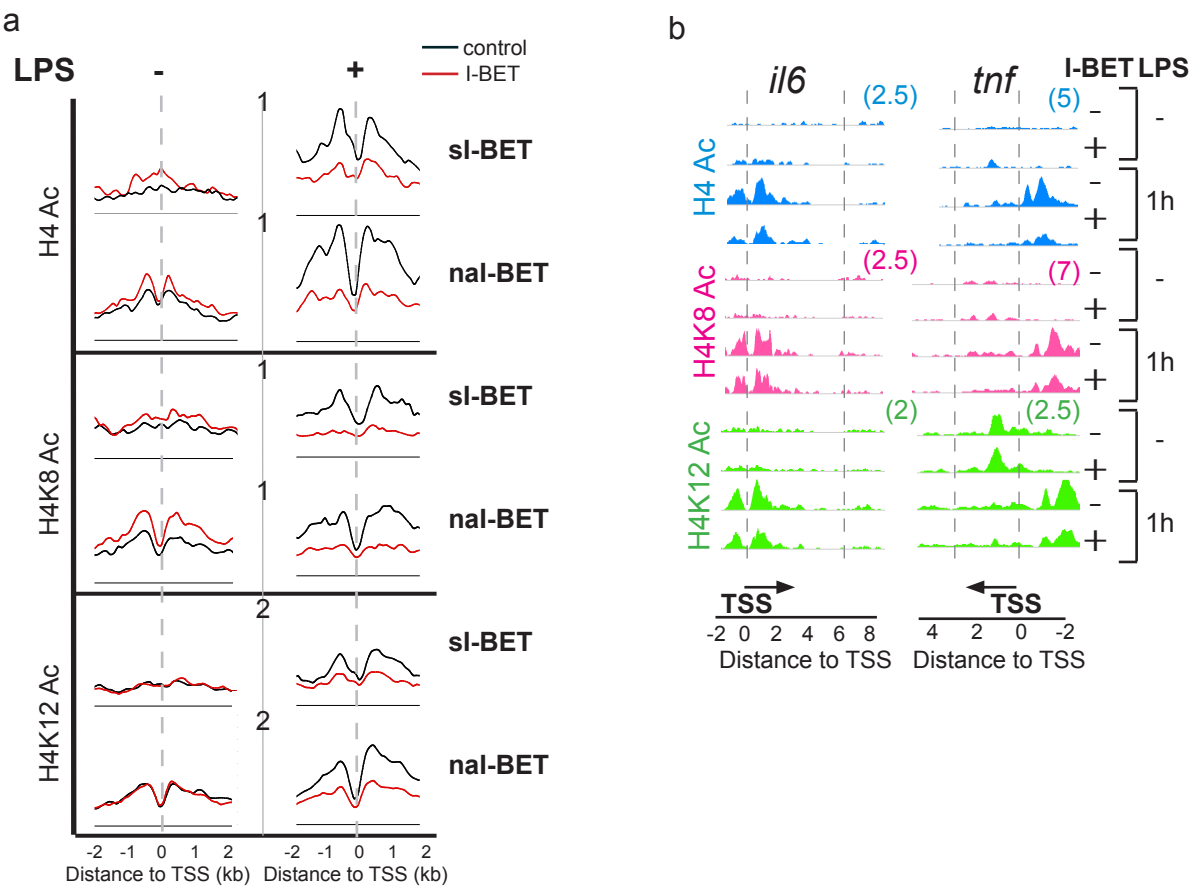

Supplementary Figure 8. Acetylation states of histone H4 at genes suppressed (sI-BET) or not affected (nal-BET) by I-BET in LPS-stimulated macrophages. a, BMDMs were pre-incubated with 5 M of I-BET (red) or DMSO as a control (black) for 30 minutes and left untreated or were stimulated with LPS (100 ng/mL) for 1 hour. Integrated genome-wide profiles of H4Ac, H4K8Ac and H4K12Ac enrichment at LPS-inducible genes suppressed by I-BET (sI-BET) or genes not affected by I-BET (nal-BET) at 1 hour after LPS stimulation are shown. The abundance of modified histones was determined by ChIP sequencing and integrated enrichment values for each sample were obtained by calculating the average enrichment value for specific sets of genes (sI-BET or nal-BET) in 100bp bins upstream and downstream of the transcriptional start site (TSS) for the distance indicated. The y axes represent the number of reads per million mapped reads and dotted grey lines indicate the TSS. **b,** H4Ac, H4K8Ac, H4K12Ac profiles of *il6* and *tnf* genes in unstimulated or LPS-stimulated BMDMs that were pre-treated with DMSO as a control (-) or with 5 M of I-BET (+). The y axes represent the average number of tags per gene per 25 bp per 1,000,000 mapped reads. Scale values are indicated in parentheses and dotted grey lines indicate the gene body.

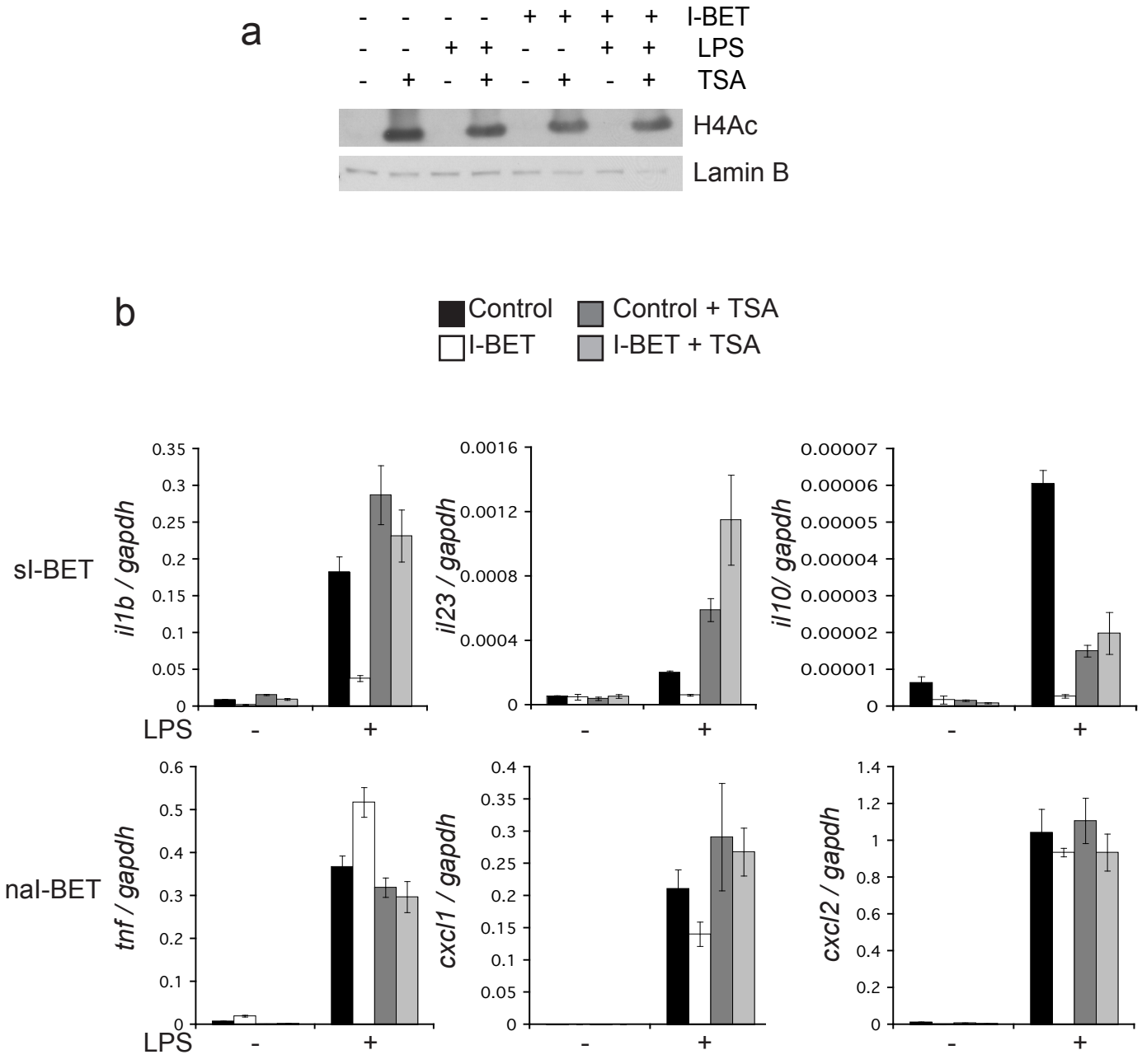

Supplementary Figure 9. Inhibition of histone deacetylases (HDACs) by trichostatin A converts sI-BET into naI-BET genes. **a,** Trichostatin A (TSA) treatment of macrophages increases global H4 acetylation. Macrophages were incubated with trichostatin A (TSA, 400 nM, Cell Signalling #9950) or ethanol for 6 hours, followed by treatment with I-BET (5 μM) or DMSO for 30 minutes and were left un-stimulated or stimulated with LPS (100 ng/mL) for 1 hour. Global levels of H4Ac were determined by Western blot analysis of whole cell lysates, only a short exposure is shown (note: H4Ac in non TSA-treated cells was detected after a longer exposure). Protein loading was determined by immunoblotting for Lamin B. **b,** Inhibition of HDACs converts sI-BET into naI-BET genes. Expression levels of the indicated genes was determined by qPCR. Bars are coloured according to the conditions used in the experiments. The value of gene expression was normalised to the expression levels of *gapdh*. Data shown are the mean of three independent experiments. Error bars represent s.e.m.

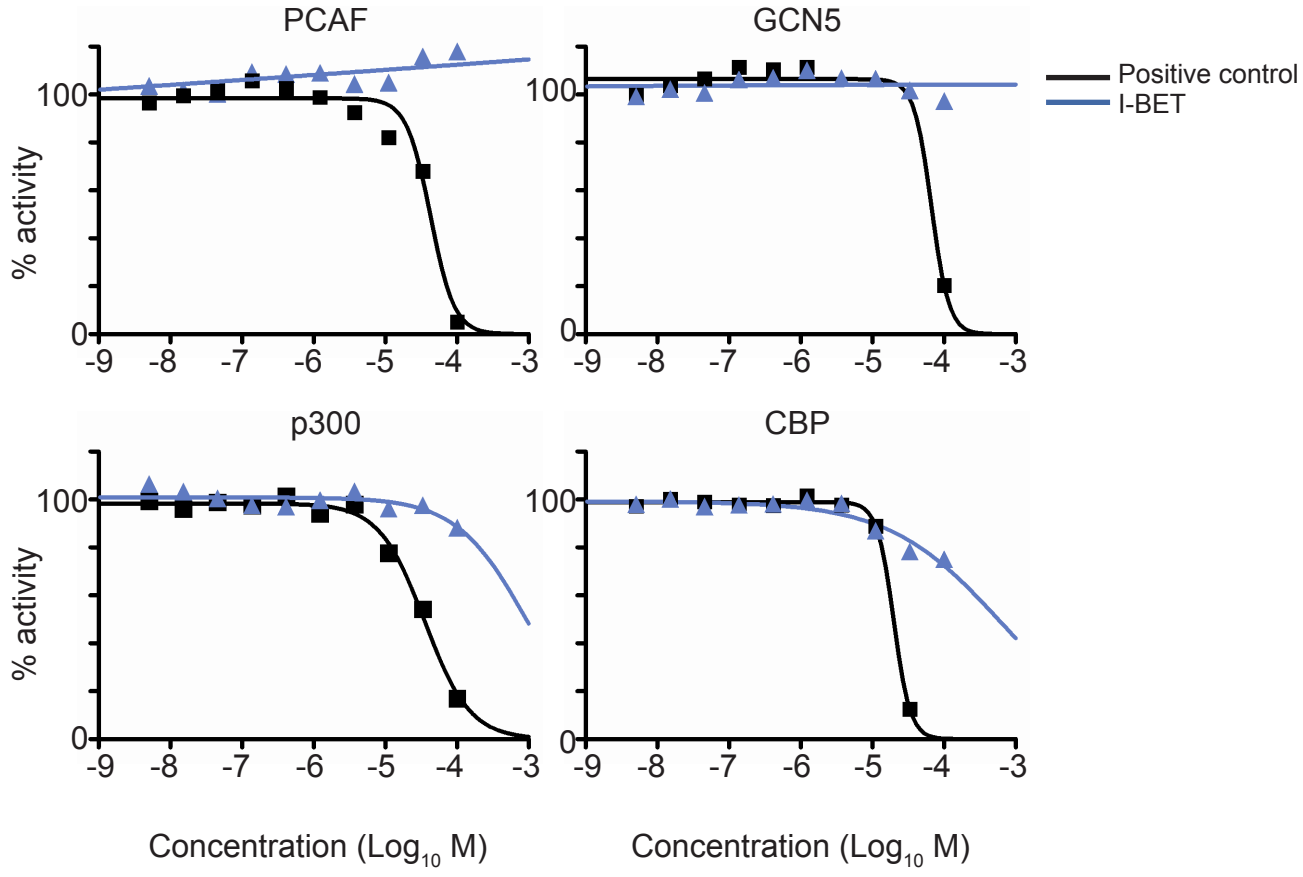

Supplementary Figure 10. I-BET has no activity towards histone acetyltransferases. The effect of I-BET on the catalytic activity of pCAF, GCN5, p300 and CBP was determined by HotSpot HAT activity assay (Reaction Biology Corporation) according to the standard operating procedure. In brief, the recombinant catalytic domains of pCAF (aa 492-658), GCN5 (aa 497-663), p300 (aa 1284-1672) or CBP (aa 1319-1710) were incubated with histone H3 as a substrate and [Acetyl-3H]-Acetyl Coenzyme A as an acetyl donor in reaction buffer (50 mM Tris-HCl (pH 8.0), 50 mM NaCl, 0.1 mM EDTA, 1 mM DTT, 1 mM PMSF, 1% DMSO) for 1 hour at 30°C in the presence or absence of I-BET at indicated concentrations. Histone H3 acetylation levels were determined by measuring the amount of the radioactively-labeled histone H3 . Anacardic acid or curcumin that inhibit pCAF, GCN5 and CBP or p300 activity, respectively, were used as positive controls. Data was analyzed using Excel and GraphPad Prism software for IC_{50} curve fits.

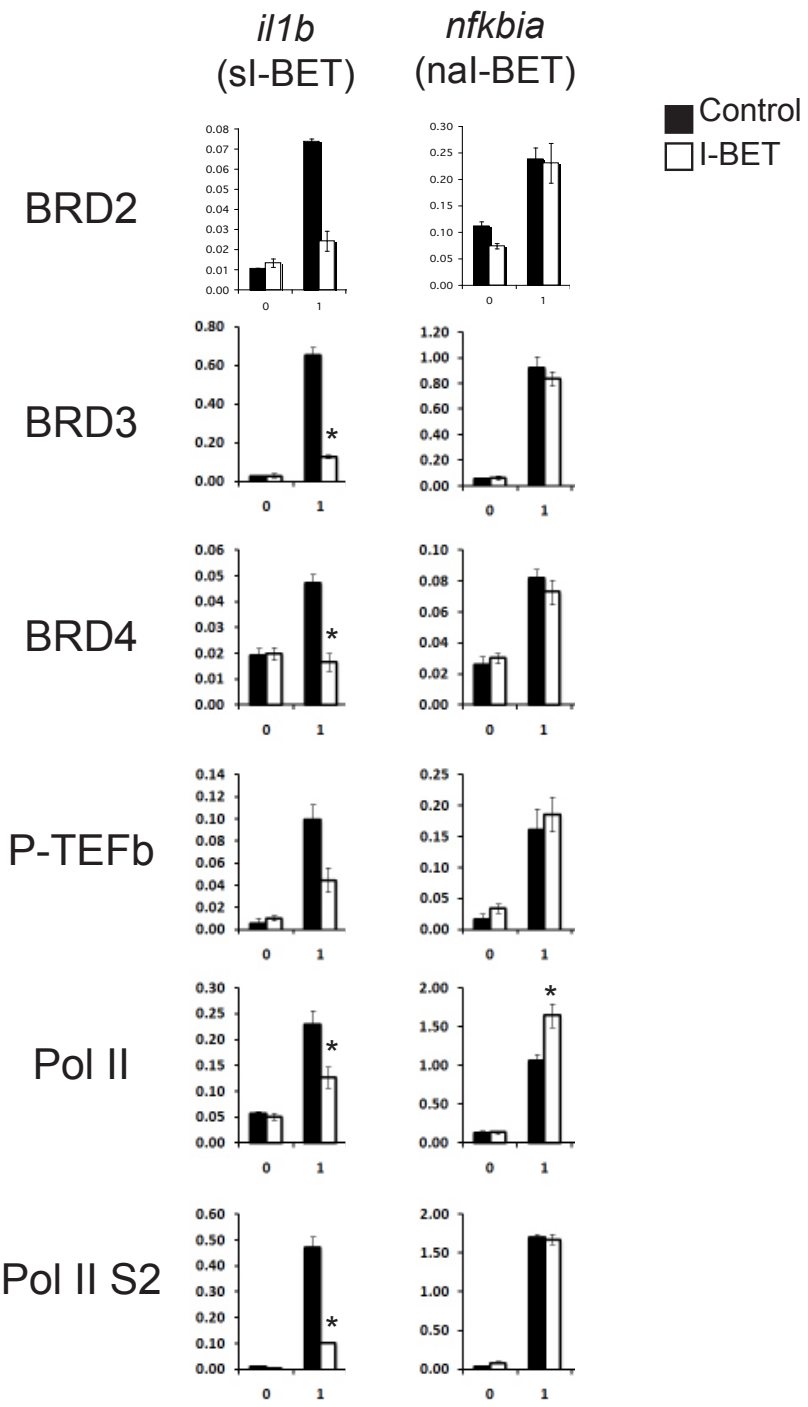

Supplementary Figure 11. I-BET prevents binding of BRD2, BRD3 and BRD4 and recruitment of P-TEFb and Pol II to sI-BET, but not to naI-BET genes. Quantitative analysis of the epigenetic states of *il1b* (sI-BET) and *nfkbia* (naI-BET) promoters in BMDMs. BMDMs were stimulated with LPS for 1 hour following pre-treatment with DMSO (black bars) or 5 μM of I-BET (white bars). The abundance of epigenetic marks was determined by ChIP qPCR. For BRD3, BRD4, Pol II and Pol II S2 the data show the results obtained from three to four independent experiments performed in triplicate. Error bars are s.e.m. of independent experiments. BRD2 and P-TEFb are representative of two independent experiments performed in triplicate. Error bars are s.d. of the triplicate. Asterisk indicate $p<0.05$ as determined by an unpaired T-test.

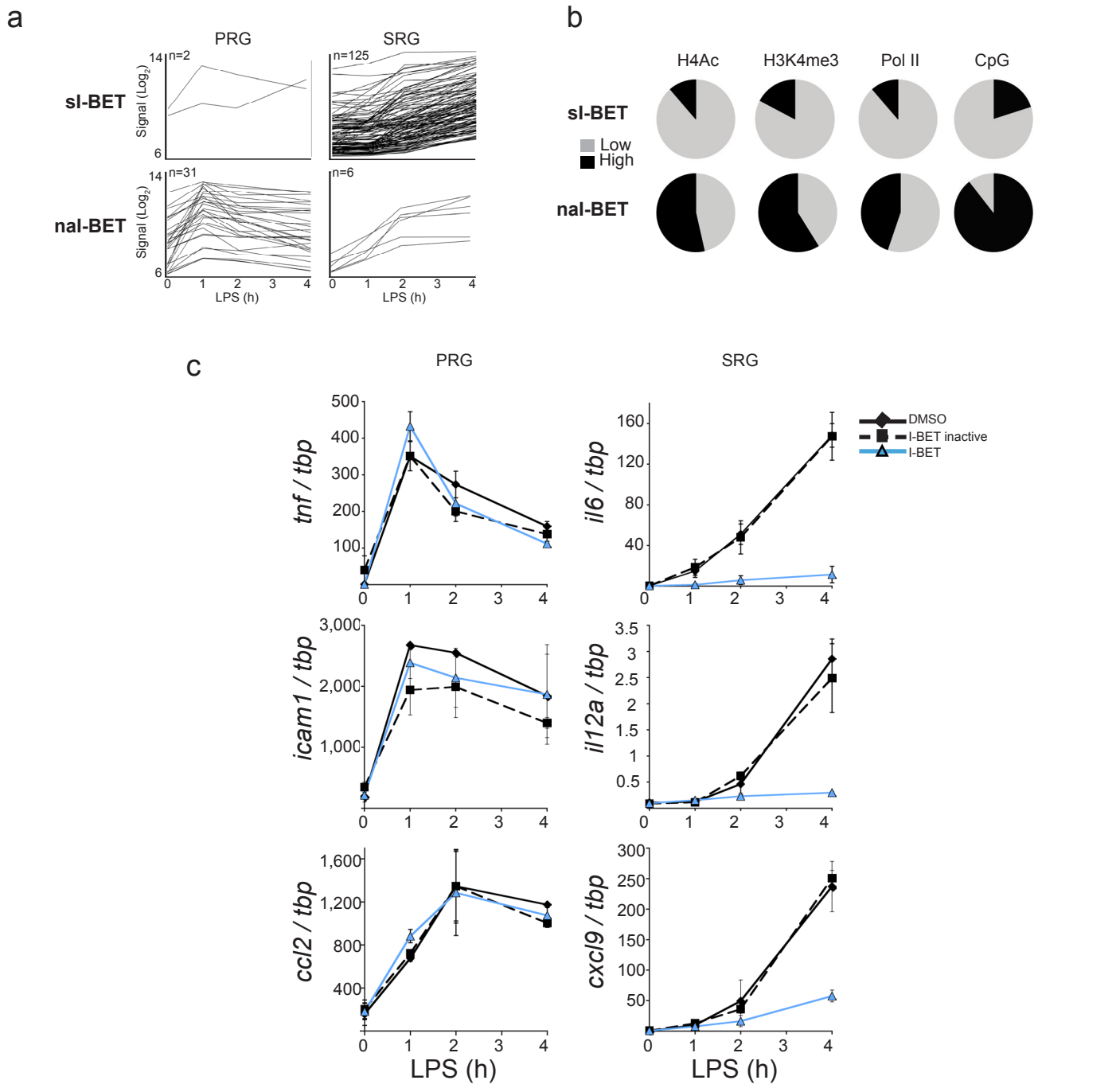

Supplementary Figure 12. I-BET suppresses secondary response genes in LPS-stimulated macrophages. a, The temporal pattern of sI-BET and naI-BET gene expression after LPS stimulation. Each line follows the kinetics of mRNA levels for an individual gene. Gene expression levels were measured by microarray and the temporal patterns of individual genes were established by using an algorithm written in R (http://www.r-project.org/) to classify genes as either Primary Response Genes ('PRGs') or Secondary Response Genes ('SRGs'). **b,** Pie charts show the proportion of genes with the following epigenetic characteristics at their promoter that are typical for SRGs (Hargreaves *et al*, 2009; Ramirez-Carrozzi *et al*, 2009): $H4Ac_{low}$, $H3K4me3_{low}$, Pol II_{low} and CpG_{low} (grey) among sI-BET or naI-BET genes in resting macrophages. Peak values for each histone modification or promoter-bound protein in unstimulated cells were determined by calculating the normalized enrichment value within specific windows surrounding the TSS as follows: -2kb to +2kb for H4Ac; -300bp to +700bp for total Pol II; -1kb to +3kb for H3K4me3. The arithmetic mean for all the enrichment values of affected and unaffected genes at 0 hours was calculated. Genes with enrichment above this value were classified as 'high' (black), those below as 'low' (grey). CpG content analysis was determined by using data from Ramirez-Carrozzi *et al*, 2009. **c,** Differential sensitivity of primary and secondary response genes to I-BET. BMDMs were pre-treated with 1 μM of I-BET (blue triangles), an inactive enantiomer of I-BET (black squares, dashed line) or DMSO as a control (black diamonds) for 30 minutes before LPS stimulation (100 ng/mL) for indicated time periods. Gene expression levels were measured by qPCR. Data are the average of 3 independent experiments. Error bars represent the s.e.m.

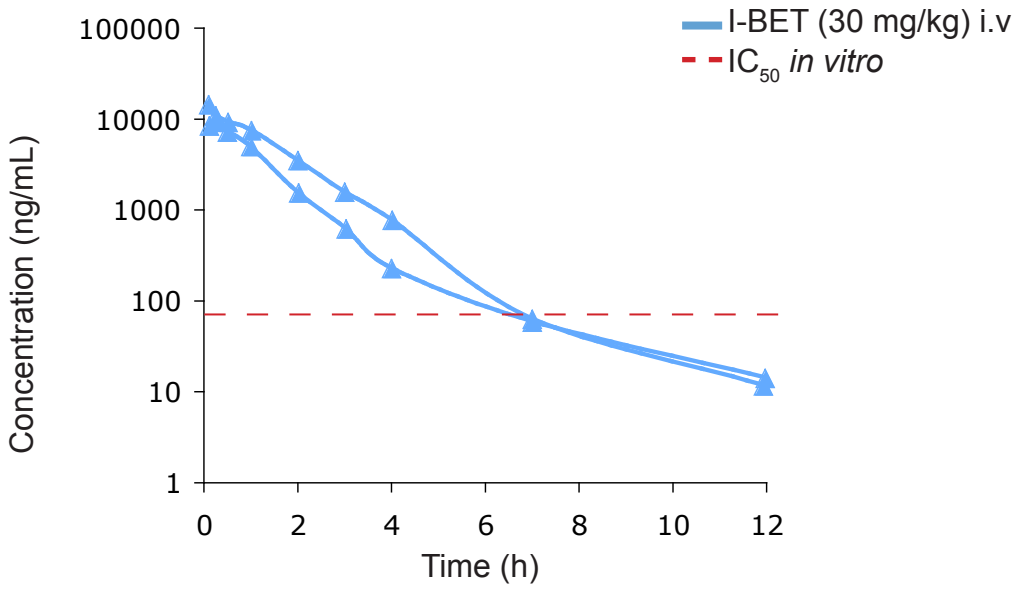

Supplementary Figure 13. Pharmacokinetics of I-BET *in vivo*. Mice were injected with I-BET via a tail vein at a dose of 30 mg/kg. The concentrations of I-BET in blood samples, drawn at different time points after injection, were determined by reverse phase HPLC using an Ascentis Express C18 column after acetonitrile protein precipitation and levels of I-BET were measured using a specific MS/MS method employing a heat assisted electrospray interface in positive ion mode (PE SCIEX API 4000). Pharmacokinetic data analysis was undertaken using WinNonlin v4.1a software. Blue lines indicate individual mice. Red dotted line indicates IC_{50} of I-BET *in vitro*.

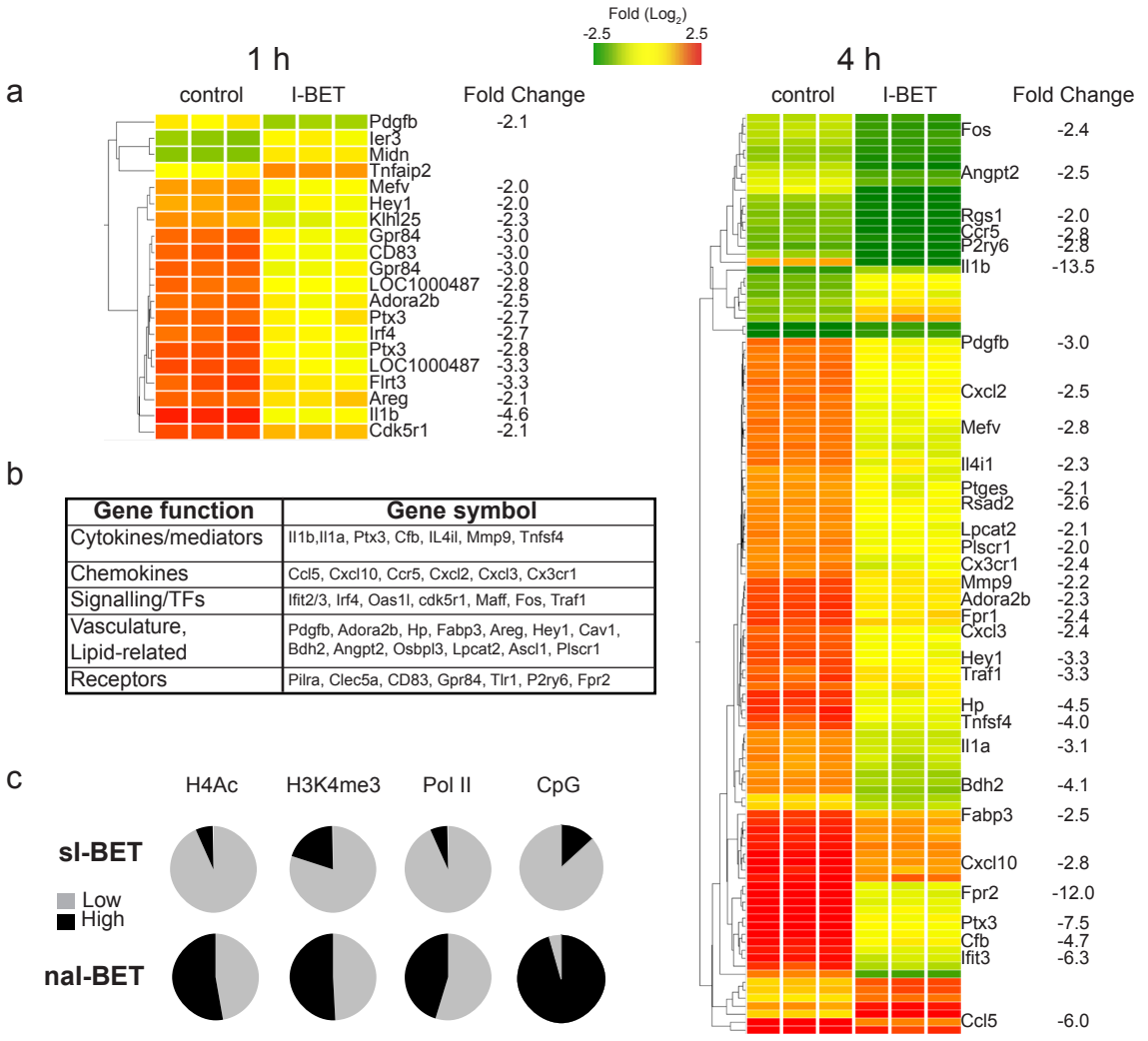

Gene function	Gene symbol
Cytokines/mediators	Il1b,Il1a, Ptx3, Cfb, IL4il, Mmp9, Tnfsf4
Chemokines	Ccl5, Cxcl10, Ccr5, Cxcl2, Cxcl3, Cx3cr1
Signalling/TFs	Ifit2/3, Irf4, Oas1l, cdk5r1, Maff, Fos, Traf1
Vasculature, Lipid-related	Pdgfb, Adora2b, Hp, Fabp3, Areg, Hey1, Cav1, Bdh2, Angpt2, Osbpl3, Lpcat2, Ascl1, Plscr1
Receptors	Pilra, Clec5a, CD83, Gpr84, Tlr1, P2ry6, Fpr2

Supplementary Figure 14. I-BET suppresses the TNF-inducible gene expression. a, Heatmap representation of TNF inducible genes that were down-regulated or up-regulated (>2-fold) by I-BET at 1 hour (left panel) or 4 hours (right panel) after TNF (50 ng/mL) stimulation of macrophages. Scale ranges are indicated. Fold change values of gene expression are listed. **b,** Distribution of down-regulated genes into functional categories. **c,** The proportion of genes with low (grey) or high (black) basal levels of H4Ac, H3K4me3, Pol II and CpG content among the TNF inducible sI-BET and naI-BET genes. Peak values for each histone modification or promoter-bound protein in unstimulated cells were determined by calculating the normalized enrichment value within specific windows surrounding the TSS as follows: -2kb to +2kb for H4Ac; -300bp to +700bp for total Pol II; -1kb to +3kb for H3K4me3. The arithmetic mean for all the enrichment values for affected and unaffected genes at 0 hours was calculated. Genes with enrichment above this value were classified as 'high' (black), those below as 'low' (grey). CpG content analysis was determined by using data from Ramirez-Carrozzi *et al*, 2009.

Supplementary Table 1. I-BET selectivity assays. I-BET activity was tested against a range of protein types using indicated functional assays. Highlighted proteins had an IC_{50} greater than 5 (10 M). N is the number of replicates.

TARGET CLASS	TARGET	ASSAY	IC50 (-log 10)	N
BROMODOMAIN	BRD2 (Bromodomain 2)	Human FP binding	6	17
BROMODOMAIN	BRD3 (Bromodomain 3)	Human FP binding	6.4	19
BROMODOMAIN	BRD4 (Bromodomain 4)	Human FP binding	6.3	19
BROMODOMAIN	BRD4 (Bromodomain 4)	Human TR-FRET Peptide Binding	6.8	2
ENZYME	Cyclooxygenase 2 (COX-2)	Human inhibition FLINT	<4	12
ENZYME	Cytochrome P450 2C19	Human inhibition FLINT	<4.3	1
ENZYME	Cytochrome P450 2C9	Human inhibition FLINT	<4.3	1
ENZYME	Cytochrome P450 2D6	Human inhibition FLINT	<4.3	1
ENZYME	Cytochrome P450 3A4	Human Vivid Green inhibition FLINT	<4.3	1
ENZYME	Cytochrome P450 3A4	Human Vivid Red inhibition FLINT	<4.3	1
ENZYME	Human Monoamine Oxidase (MAO) B	Human inhibition FLINT	4.6	3
ENZYME	PDE4B (cAMP-specific 3',5'-cyclic phosphodiesterase 4B)	Human inhibition luminescence	<4.6	6
GPCR	5-HT Transporter (5-hydroxytryptamine transporter, SERT, serotonin transporter)	Human SPA binding	4.2	1
GPCR	5-HT1B (5-hydroxytryptamine receptor 1B)	Human antagonist GTPgS	<4	12
GPCR	5-HT2A (5-hydroxytryptamine receptor 2A)	Human antagonist intracellular Ca^{2+} luminescence	<4.4	12
GPCR	5-HT2C (5-hydroxytryptamine receptor 2C)	Human antagonist intracellular Ca^{2+} luminescence	<4.4	12
GPCR	Adrenergic Alpha 1B	Human antagonist intracellular Ca2+ fluorescence	<4.4	6
GPCR	Beta2 Adrenoceptor	Human antagonist TR-FRET	<4.5	12
GPCR	Dopamine 2 (D2)	Human antagonist GTPgS	<4	6
GPCR	Dopamine 1 (D1)	Human antagonist TR-FRET	<4.5	6
GPCR	Histamine Receptor H1 (HRH1)	Human antagonist intracellular Ca^{2+} luminescence	<4.4	12
GPCR	5-HT3 (5-hydroxytryptamine receptor 3)	Human antagonist intracellular Ca2+ fluorescence	<4.3	6
GPCR	M1 (Muscarinic acetylcholine receptor M1)	Human antagonist intracellular Ca2+ fluorescence	<4.82	12
GPCR	M2 (Muscarinic acetylcholine receptor M2)	Human antagonist intracellular Ca2+ fluorescence	<4.8	14
GPCR	NK1 (Tachykinin receptor 1)	Human antagonist intracellular Ca^{2+} luminescence	<4.4	11
GPCR	OPRK1 (kappa Opioid receptor 1)	Human antagonist GTPgS	<4	6
GPCR	OPRM1 (mu Opioid receptor 1)	Human antagonist GTPgS	<4	6
GPCR	Vasopressin (V1a)	Human antagonist intracellular Ca2+ fluorescence	<4.3	6
ION CHANNEL	Alpha 1 nAChR (Nicotinic acetylcholine receptor)	Human blocker intracellular Ca2+ fluorescence	4.8	6
ION CHANNEL	CaV1.2 (Calcium channel, voltage-dependent, L type, alpha 1C subunit)	Human blocker intracellular Ca2+ fluorescence	<4.8	9
ION CHANNEL	hERG (Kv11.1 potassium ion channel)	Human blocker PatchXpress	4.2	1
ION CHANNEL	hERG (Kv11.1 potassium ion channel)	Human FP binding	<4	13
ION CHANNEL	KCNQ1/KCNE1 (voltage-gated potassium ion channel QKT subfamily member 1)	Human Blocker ionworks	4.6	1
ION CHANNEL	Kv1.5 (KCNA5, voltage-gated potassim ion channel, shaker-related subfamily, member 5)	Human Blocker ionworks	<4.3	6
ION CHANNEL	NaV1.5 (voltage-gated sodium ion channel, type V)	Human Blocker ionworks	<4	5
KINASE	Aurora B kinase	Human inhibition FP binding	<4.6	6
KINASE	GSK3β (Glycogen synthase kinase 3 beta)	Human FP binding	<4.6	6
KINASE	LCK (Lymphocyte-specific protein tyrosine kinase)	Human inhibition FP binding	<4.6	6
KINASE	PI3K-γ (Phosphoinositide 3-kinase gamma)	Human inhibition TR-FRET	<4.6	6
TRANSPORTER	Dopamine Transporter (DAT)	Human SPA binding	4.1	1
TRANSPORTER	Noradrenaline Transporter (NET)	Human SPA binding	<4	6
TRANSPORTER	Organic Anion Transporting Polypeptide C (OATP1B1)	Human inhibition FLINT imaging	4.9	4

Supplementary Table 2. A summary of I-BET effects on gene expression in LPS-stimulated macrophages. BMDMs were pre-treated either with 1μM of I-BET or with DMSO as a control and were left un-stimulated or were stimulated for 1 or 4 hours with 100 ng/mL of LPS. The analysis was performed in triplicate. Gene expression levels were analyzed by microarray (Illumina). The sI-BET genes, naI-BET genes and genes up-regulated by I-BET are listed.

Unstimulated		LPS 1h			LPS 4h		
Up-regulated with I-BET >2 fold	**Down-regulated with I-BET >2 fold**	**Up-regulated with I-BET >2 fold**	**1h Down-regulated with I-BET >2 fold (LPS-induced > 2 fold) sI-BET**	**1h Unaffected (LPS induced only) naI-BET**	**Up-regulated with I-BET >2 fold**	**1h Down-regulated with I-BET >2 fold (LPS-induced > 2 fold) sI-BET**	**4h Unaffected (LPS induced only) naI-BET**
Hist1h2ac	none	Bzrap1	A630077B13Rik	Axud1	1110028C15Rik	100042856	1110038F14Rik
Hist1h3a		Ccno	Areg	Bcl2l11	1810055G02Rik	1200009O22Rik	1190005F20Rik
Hist1h3d		Dalrd3	Arg2	Ccl2	2610024G14Rik	6330442E10Rik	1200009I06Rik
Hist1h3f		Dnajb1	Bcl6	Ccl4	Adamts4	9930022N03Rik	1200015F23Rik
Hist1h3h		Dusp2	Cav1	Ccng2	Adrb2	9930111J21Rik	1300018I05Rik
Hist1h4f		Egr4	Ccl5	Ccnl1	Agrn	A630077B13Rik	1700047I17Rik1
Hist1h4h		Fosb	Cd83	Cd14	Amd-ps3	Acsl1	2810012G03Rik
Hist1h4i		Gadd45b	Cdk5r1	Cd40	Asah3l	Adm	3110009E18Rik
Hist1h4j		Gadd45g	Ch25h	Cd44	Bcor	Aftph	3300001P08Rik
Hist1h4k		Hist1h3a	Cxcl10	Cd69	Bzrap1	AI451617	4632411B12Rik
LOC100041230		Hist1h3d	Dusp4	Cdc42ep2	C230093N12Rik	Aldh1b1	4921505C17Rik
		Hist1h3h	Edn1	Cish	Ccdc85b	Apobec3	4930453N24Rik
		Hist1h4f	EG622976	Cited2	Cd3eap	Apol7c	4933426M11Rik
		Hist1h4i	Flrt3	Clcf1	Cdan1	Apol9b	5730596K20Rik
		Hist1h4j	Fpr2	Cxcl1	Centb5	Arg2	6330409N04Rik
		Hist2h3b	Gja1	Cxcl2	Chchd7	Atp10a	9030625A04Rik
		Ier3	Gpr84	Dusp1	Chd4	Axud1	A030007L17Rik
		Jun	Gpr85	Egr1	Csrnp2	Batf2	A530023O14Rik
		Klf2	H2-M2	Egr2	Ctr9	BC006779	AA467197
		LOC100044024	Ifnb1	Ehd1	Dynll1	BC094916	AA960436
		Matn4	Il10	Errfi1	Egr1	Bcl6	Abcb1b
		Midn	Il1b	Ets2	Eif4ebp2	Car4	Acvr1
		Polg2	Il23a	Frmd6	Erdr1	Cav1	Adar
		Sertad1	Il6	Gadd45a	Fbxl15	Ccl12	Aebp2
		Tsc22d3	Inhba	Gbp5	Frmd6	Cd200	Aff1
		Txnip	Irf4	Hspa1a	Gadd45a	Cd69	AI118078
			Isg15	Icam1	H2afx	Cd80	Aida
			Klhl25	Irf1	Hexim1	Cd86	Akap2
			LOC100045233	Jmjd3	Hist1h1c	Cfb	Akna
			Pcdh7	Junb	Hist1h2bc	Ch25h	Amigo3
			Ptx3	Klf6	Hist1h2bf	Clec5a	Ankrd17
			Rel	LOC100040573	Hist1h2bh	Cp	Ap3m2
			Rgs1	Maff	Hist1h2bk	Creb5	Arhgef3

Serpinb2	Malt1	Hist1h2bm	Cst7	Asb13
Skil	Map3k8	Hist1h2bn	Cxcl9	Batf
Slc7a11	Marcksl1	Hist1h3a	D14Ertd668e	Bcl2a1d
Tnfsf4	Mdm2	Hist1h3d	Dennd3	Bcl2l11
Traf1	Mx2	Hist1h3f	Dhx58	Bcl3
	Myd116	Hist1h3h	Dnaja2	Bfar
	Nfkbid	Hist1h4f	Ebi3	Birc2
	Nfkbie	Hist1h4h	Edn1	Bmp1
	Nfkbiz	Hist1h4i	Epsti1	C3
	Pim1	Hist1h4j	F10	C330023M02Rik
	Pim3	Hist1h4k	Fcgr1	C5ar1
	Plk2	Hist2h3c1	Fgl2	Camkk2
	Pvr	Hrbl	Fpr1	Car13
	Rasgef1b	Hspa2	Fpr2	Ccdc25
	Rcan1	Id3	Fst	Ccdc50
	Relb	Ier3	Fzd1	Ccdc86
	Rnd3	Impact	Gbp10	Ccl2
	Sgk1	Isca1	Gca	Ccl3
	Socs3	Klf2	Gcnt2	Ccl4
	Tgif1	Klhl21	Gja1	Ccl5
	Tnf	LOC100041230	Gnb4	Ccng2
	Tnfsf9	LOC100044024	Gpr18	Ccnl1
	Trex1	LOC100046213	Gpr84	Ccrl2
	Vcam1	LOC100047260	Gpr85	Cd14
	Vegfa	LOC100047324	Gramd1b	Cd274
	Zc3h12a	Mars2	H2-M2	Cd40
	Zfp36	Mknk2	I830012O16Rik	Cd44
	Zswim4	Mrpl49	Ifi205	Cd83
		Mrps6	Ifi47	Cdc42ep2
		Msh6	Ifit3	Cdkn1a
		Napepld	Ifnb1	Cenpj
		Phlda1	Igsf9	Chd1
		Ppfia3	Igtp	Cited2
		Prei4	Ikzf1	Cldnd1
		Ptbp1	Il10ra	Clec2d
		Rbm14	Il12a	Clic4
		Rbm38	Il15ra	Cmpk2
		Slc19a2	Il19	Col27a1
		Slc25a33	Il1rn	Cox18
		Slc35e3	Il23a	Cpd
		Slc7a5	Il27	Cpd
		Snora65	Il33	Crkl
		Sqle	Il6	Csf1

Ssbp3	Inhba	Cx3cl1
Tmem41a	Irf8	Cxcl1
Tob1	Isg20	Cxcl10
Tsc22d3	Klf7	Cxcl16
Tubb2c1	Klrk1	Cxcl2
Txnip	Kynu	D16Ertd472e
Ube2o	Lad1	D17Wsu92e
Usp20	Lck	Daam1
Wdr75	Lcn2	Daxx
Zfp36	Lhx2	Dbnl
Zfp672	LOC100038946	Dcbld2
Zfyve21	LOC100046788	Dcp1a
	LOC435565	Ddhd1
	LOC625360	Ddx24
	LOC637605	Denr
	Lrch1	Dst
	Ly6c1	Dtx2
	Mefv	Dusp11
	Mfsd7	Dusp2
	Mid1	Dusp28
	Mitf	E130012A19Rik
	Mmp13	E2f3
	Mmp14	E2f5
	Mmp2	EG666726
	Mtus1	Eml4
	Mycl1	Ep400
	Nos2	Ets2
	Oas1a	Ext1
	Oas2	Fbxw17
	Oas3	Fchsd2
	Oasl2	Fmo3
	Osbpl3	Foxp4
	P2ry13	Gbp2
	P2ry14	Gbp5
	Pcdh7	Gch1
	Pdcd10	Gmppb
	Phf11	Gna13
	Pilra	Gosr2
	Pilrb1	Gpd2
	Pla1a	Gtf2f1
	Ptgs2	H2-T10
	Ptx3	Hamp
	Pvrl2	Hif1a

Rasgrp1	Hisppd1
Rdh11	Icam1
Rilpl1	Ifi203
Saa3	Ifnar2
Samd9l	Igsf3
Sbno2	Il15
Schip1	Il20rb
Serpina3f	Il4i1
Serpina3g	Irak3
Serpinb2	Irf1
Sipa1l1	Irf5
Slamf1	Isg15
Slc1a2	Itga5
Slc28a2	Itgav
Slc7a11	Jak2
Slfn1	Jdp2
Smpdl3b	Jmjd2a
Spsb1	Katna1
Tcf4	Kif1b
Tgtp	Kpna3
Tlr3	Kremen1
Tlr6	Krit1
Tmem132e	Lcp2
Tnfsf10	Lmo4
Tnfsf15	LOC100044021
Tnfsf4	LOC100044206
Traf1	LOC100044233
Tsc22d1	LOC100047963
Ube1l	LOC192690
Upp1	Mafk
Zbtb8a	Malt1
Zeb1	Map2k1
	Map3k7ip2
	Map3k8
	Mapk1ip1l
	Mapkapk2
	Mapkbp1
	Marcks
	Mdk
	Mfsd7
	Morc3
	Mt2
	Mtmr14

Mx1
Mx2
Nampt
Nat2
Ncoa5
Nfkb1
Nfkb2
Nfkbib
Nfkbie
Nfkbiz
Nrap
Nrp2
Nupr1
Oas1b
Oasl1
Ogfr
Optn
Palld
Papd4
Parp14
Pcgf3
Pde4b
Pdss1
Peli1
Phc2
Phldb1
Pim1
Pkn2
Plagl2
Plcb3
Plk2
Plscr1
Pou3f1
Ppa1
Ppap2a
Ppap2b
Ppm1b
Ppm1k
Ppp1r10
Ppp1r15b
Ppp2r5a
Prdx5
Prpf38a

Psmb8
Psmb9
Pstpip2
Ptprj
Pvr
Rab12
Rab32
Rab38
Ranbp2
Rars
Rassf4
Rcl1
Rel
Rela
Relb
Rffl
Rhbdf1
Rhbdf2
Rhou
Ripk2
Rnd3
Rnf114
Rnf135
Rnf145
Rnf31
Rod1
Rsad2
Sap30
Saps1
Sertad1
Sgcb
Sgms2
Sh3bgrl2
Slc16a10
Slc25a37
Slc2a6
Slc3a2
Slc7a8
Slco3a1
Slfn2
Slfn5
Smg7
Snn

Snx20
Socs3
Sod2
Sqstm1
St3gal1
St3gal3
Stard5
Stat1
Stat2
Stat5a
Stau1
Stk40
Stxbp1
Swap70
Syf2
Tdrd7
Tfg
Tgm2
Tifa
Timp1
Timp3
Tlr2
Tmem2
Tmem39a
Tmprss11d
Tnc
Tnf
Tnfaip3
Tnfrsf1b
Tnip1
Tor1aip1
Tor1aip2
Tra2a
Traf5
Trafd1
Trex1
Trim21
Trim26
Triobp
Trip10
Ttc39c
Ube2f
Usp18

	Usp25
	Vcam1
	Vcpip1
	Vps54
	Wdr37
	Xkr8
	Ythdf1
	Zbtb5
	Zc3h12a
	Zc3h7a
	Zfp281
	Zfp295

Supplementary Table 3. A summary of the effect of I-BET on gene expression in resting macrophages.
BMDMs were treated with 1 μM of I-BET or DMSO as a control and gene expression was determined by microarray (Illumina). Genes up-regulated or down-regulated by I-BET (>2-fold) are shown.

I-BET 1.5 h				I-BET 4.5 h			
I-BET up-regulated >2 fold		**I-BET down-regulated >2 fold**		**I-BET up-regulated >2 fold**		**I-BET down-regulated >2 fold**	
Bzrap1	4.93	Ch25h	4.22	Hist1h4f	4.64	Galnt9	6.19
Hist1h3d	4.90	Flrt3	4.20	Hist1h3e	4.45	Hr	3.82
Hist1h3a	4.59	Inhba	4.04	Hist1h3d	4.43	LOC100048556	3.50
Hist1h3e	4.17	LOC100048721	3.83	Brd2	4.00	Ch25h	3.33
Brd2	3.86	Il1b	3.27	Hist1h2bc	3.96	Fcgr1	3.32
Hist1h4f	3.38	Gja1	3.12	Hist1h4j	3.87	Sh2d1b1	3.16
Brd2	3.34	Cytip	3.05	Hist1h2bk	3.76	Fblim1	3.14
Hist1h4i	2.97	Fbxo32	2.97	Bzrap1	3.76	Ccnd1	3.12
Hist1h2bm	2.76	LOC100048556	2.89	Hist1h4i	3.73	Kcnn4	3.06
Hist1h2bk	2.68	Pdgfb	2.79	Hist1h4h	3.68	Egr2	3.00
Hist1h4h	2.62	Gpr109a	2.75	Hist1h2bj	3.53	Angptl4	2.95
Hist1h2bc	2.57	Zfp608	2.73	Hist1h2bm	3.51	Sla	2.90
Hist1h2bh	2.56	Cd86	2.68	Brd2	3.35	Rnase6	2.86
Hist1h4j	2.55	Fbxo32	2.63	Hist1h3a	3.33	LOC100048556	2.80
Hist1h2bj	2.52	Galnt9	2.53	Hist1h2bh	3.30	Ptpro	2.78
Hist1h4m	2.50	Cd86	2.52	Hist1h4k	3.29	Ciita	2.78
Brd2	2.49	Cd83	2.51	Brd2	3.24	Mcf2l	2.77
Hist1h2bf	2.48	Satb1	2.51	Hist1h2bn	3.18	Ccnd1	2.75
Egr1	2.47	LOC100048556	2.40	Hist2h3c1	3.13	Gja1	2.74
Hist1h1c	2.46	Gpr120	2.40	Hist1h4m	3.12	Inhba	2.70
Hexim1	2.45	Ccrl2	2.39	Hist1h1c	3.00	Oit3	2.70
Hist1h2bn	2.42	Arg2	2.36	Hist1h2bf	2.98	P2ry13	2.69
Hist1h4k	2.39	Ptger2	2.35	Hexim1	2.98	Gpr120	2.68
Rbm15	2.29	Creb5	2.32	LOC100047261	2.59	Havcr2	2.64
Hist1h2ac	2.14	Gpr85	2.32	Nfkbiz	2.53	Slco2b1	2.64
Hist3h2a	2.13	Nrg1	2.27	Hist2h3b	2.48	Tm7sf4	2.61
Fzd5	2.12	Egr2	2.25	Hist1h2bc	2.48	Havcr2	2.61
Polg2	2.11	Fos	2.22	Hist2h3c1	2.43	Dnmt3l	2.55
H3f3b	2.08	Pus3	2.17	Ier3	2.29	Slamf8	2.54
Hist1h2bg	2.06	Tnfsf14	2.13	Hist1h2bg	2.23	Angpt2	2.51
		Foxq1	2.13	Fbxl4	2.23	Dnmt3l	2.43
		Crem	2.11	Rpe	2.22	Scel	2.42
		Gdf15	2.08	Cirbp	2.18	Ptgir	2.40
		Ptger2	2.04	Ahi1	2.15	Tlr13	2.40
		Hr	2.02	Nsun4	2.06	Fos	2.34
		Prr15	2.02	Sgcb	2.04	Il1b	2.33
		2310016C08Rik	2.01			Cdh1	2.30
						Gpr109a	2.29
						Slc7a11	2.28
						F2rl2	2.27
						1700112C13Rik	2.25
						Cytip	2.24
						Pstpip1	2.23
						Ccr5	2.23
						Dok2	2.23
						Nr1h3	2.20
						Nags	2.20
						Pdgfb	2.19
						Pdcd1lg2	2.19
						Ccr5	2.18
						Tgfbi	2.18
						Epb4.1l1	2.18
						A430084P05Rik	2.18
						Plau	2.18
						Flrt3	2.17
						Ptpn22	2.17
						Creb5	2.17
						P2ry14	2.14
						Cd86	2.13

Il1rn	2.13
Rgs1	2.13
Blnk	2.12
H2-M2	2.12
Igfbp5	2.11
Atg9b	2.11
LOC100048721	2.11
6330442E10Rik	2.08
Gdf15	2.07
B430306N03Rik	2.07
Mcf2l	2.06
Rufy1	2.06
Cav1	2.04
5430435G22Rik	2.04
Ccr5	2.04
Klf7	2.03
Efcab4a	2.03
Sphk1	2.03
Ebi2	2.02
1110032E23Rik	2.02
Bdh2	2.01
Rsad2	1.46

METHODS:

Chemical library screen and I-BET discovery:

BET proteins (hereafter defined as BET) contribute to positive and negative regulation of gene expression[1-3]. This latter feature of BET was employed to develop a "positive" screening approach for identification of potential BET regulatory compounds. We opted for a "positive" screening approach that relies on up-regulation of gene expression due to the high number of false positive hits that are commonly generated by "negative" screening approaches that rely on down-regulation of gene or protein expression. We chose Apolipoprotein A1 (ApoA1) gene as a possible target for BET regulation. The choice of ApoA1 was based on several factors that range from the robustness of the ApoA1 reporter system to the physiological significance of ApoA1 *in vivo*. A human HepG2 hepatocyte cell line carrying the ApoA1 luciferase reporter has been used to screen a diverse compound library to identify molecules with the ability to up-regulate reporter gene activity. From this effort we identified the benzodiazepine (BZD) compound GW841819X that showed potent induction of the ApoA1 reporter gene with an EC_{50} of 440nM, and a maximum induction of 4.5 fold. GW841819X as well as the chemically related compound GSK525762A had no effect on the activity of numerous kinases, ion-channels, nuclear receptors, GPCRs and other commonly tested drug targets, including those listed in the Supplementary Table 1. To identify the compound protein targets, a derivatised version of GSK525762A was attached to a ReactiGel matrix (BZD matrix) followed by affinity chromatography of HepG2 cell lysate. A control affinity chromatography using an inactive analog was also performed. The proteins that were retained by the active BZD matrix and could be outcompeted by the addition of soluble GSK525762A, but were absent when an inactive analog or matrix alone were used, were then indentified by LC/MS/MS analysis as BET proteins BRD2, BRD3 and BRD4.

Compound characterisation for the active I-BET and an inactive enantiomer of I-BET (2-[(4 chlorophenyl)-1-methyl-8-(methyloxy)-4H-[1,2,4]triazolo[4,3-a][1,4]benzodiazepin-4-yl]-*N*-ethylacetamide)

Mp 140-145 °C; R_f = 0.48 (DCM/MeOH:90/10); ^{1}H RMN (300 MHz, $CDCl_3$) *d* 7.53-7.47 (m, 2H), 7.39 (d, *J* = 8.9 Hz, 1H), 7.37-7.31 (m, 2H), 7.20 (dd, *J* = 2.9 and 8.9 Hz, 1H), 6.86 (d, *J* = 2.9 Hz, 1H), 6.40 (m, 1H), 4.62 (m, 1H), 3.80 (s, 3H), 3.51 (dd, *J* = 7.3 and 14.1 Hz, 1H), 3.46-3.21 (m, 3H), 2.62 (s, 3H), 1.19 (t, *J* = 7.3 Hz, 3H); ^{13}C NMR (75

MHz, DMSO-d6) *d* 169.2, 165.5, 157.4, 155.8, 150.7, 137.3, 135.4, 131.0, 129.3, 128.2, 126.4, 125.6, 117.8, 115.1, 55.8, 53.3, 37.6, 33.4, 14.8, 11.5; HRMS $(M+H)^+$ calculated for $C_{22}H_{23}{}^{35}ClN_5O_2$ 424.1540; found 424.1525. HPLC using a ChiralPack AD (250 x 20 mm id, 10 µm) column eluting with EtOH/hexane (60/40) as the mobile phase (Flow rate : 17 mL/min). Active I-BET eluted at 5.21 min as the first peak. $[a]_D^{20}$ = + 88.1 (c = 1.0015 /MeOH). The inactive I-BET enantiomer came off at 24.28 min. $[a]_D^{20}$ = -87.7 (*c* 1.0015 / MeOH).

Compound synthesis of active I-BET (Cmpd1) and an inactive enantiomer of I-BET (Cmpd2) (2-[(4-chlorophenyl)-1-methyl-8-(methyloxy)-4H-[1,2,4]triazolo[4,3-a][1,4]benzodiazepin-4-yl]-*N*-ethylacetamide)

General. All commercial chemicals and solvents are reagent grade and were used without further purification unless otherwise specified. All reactions except those in aqueous media were carried out with the use of standard techniques for the exclusion of moisture. Reactions were monitored by thin-layer chromatography on 0.2 mm silica gel plates (ALUGRAM SIL G/UV254, Macherey-Nagel) and were visualized with UV light. Final compounds were typically purified either by flash chromatography on silica gel (E. Merck, 40-63 mm) or by recrystallization. ^1H and ^{13}C NMR spectra were recorded on a Bruker 300 MHz Avance DPX. Chemical shifts are reported in parts per million (ppm, d units). Splitting patterns are designed as s, singlet; d, doublet; t, triplet; q, quartet; m, multiplet; bs, broad singlet. High-resolution mass spectra were recorded on a Micromass LCT (TOF) spectrometer coupled to an analytical high performance liquid chromatography (HPLC) conducted on a XTERRA-MS C18 column (30 _ 3 mm id, 2.5 µm) eluting with 0.01 M ammonium acetate in water and 100% acetonitrile (CH_3CN), using the following elution gradient: 0 to 100% CH_3CN over 4 min and 100% CH_3CN over 1 min at 1.1 mL/min at 40 °C. Mass spectra were acquired in either positive or negative ion mode under electrospray ionization (ESI) method. Specific rotations were measured on a Perkin Elmer 343 polarimeter. Cmpds **1** and **2** were prepared using the following chemical route:

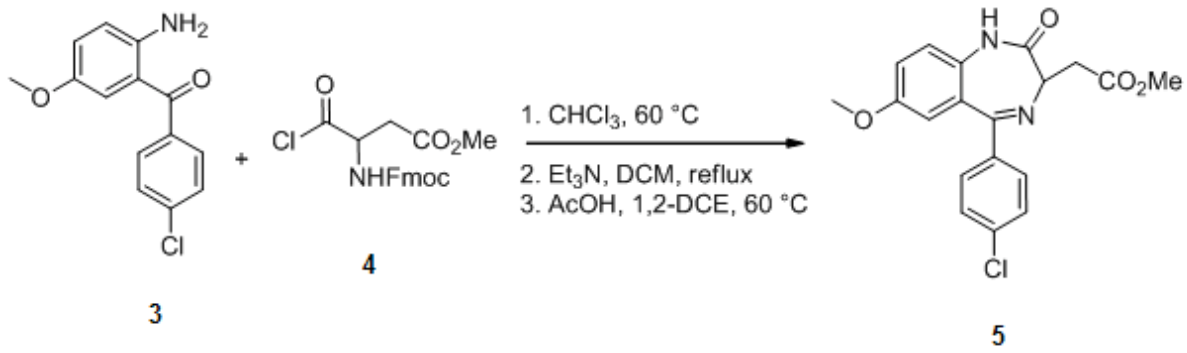

Methyl [5-(4-chlorophenyl)-7-(methyloxy)-2-oxo-2,3-dihydro-1*H*-1,4-benzodiazepin-3-yl]acetate (5)

[2-Amino-5-(methyloxy)phenyl](4-chlorophenyl)methanone **3** (3.1 g, 11.8 mmol) was added to a solution of acid chloride **4** (freshly prepared from Fmoc-aspartic acid methyl ester (4.4 g, 11.98 mmol) in $CHCl_3$ (55 mL) according to [4]. The resulting mixture was stirred at reflux for 1 hour before being cooled. Et_3N (6.6 mL, 47.4 mmol, 4 equiv.) was then added and the resulting mixture was refluxed for 16 hours before being concentrated to dryness. The resulting crude amine was dissolved in 1,2-DCE (150 mL) and AcOH (7.5 mL, 131 mmol, 11 equiv.) was added carefully. The reaction mixture was then stirred at 60°C for 1.5 hours before being concentrated *in vacuo* and dissolved in DCM. The organic layer was washed with 1N HCl and the aqueous layer was extracted with DCM (3x). The combined organic layers were washed twice with water, and brine, dried over Na_2SO_4, filtered and concentrated under reduced pressure. The crude solid was recrystallized in CH_3CN leading to the title compound **5** (1.35 g, 30% yield) as a white solid. R_f = 0.34 (DCM/MeOH:95/5). ^{1}H NMR (300 MHz, $CDCl_3$) *d* 8.73 (br s, 1H), 7.50 (m, 2H), 7.35 (m, 2H), 7.15-7.07 (m, 2H), 6.76 (m, 1H), 4.18 (dd, *J* = 7.2 and 6.8 Hz, 1H), 3.75 (s, 3H), 3.74 (s, 3H), 3.42 (dd, *J* = 16.9 and 7.2 Hz, 1H), 3.42 (dd, *J* = 16.9 and 6.8 Hz, 1H). ^{13}C NMR (75 MHz, DMSO-d6) *d* 171.6, 169.5, 166.6, 154.3, 137.1, 135.2, 132.7, 131.1, 128.4, 126.8, 122.9, 119.2, 113.4, 60.3, 55.5, 51.3, 35.9. HRMS $(M+H)^+$ calculated for $C_{19}H_{18}{}^{35}ClN_2O_4$ 373.0955; found 373.0957.

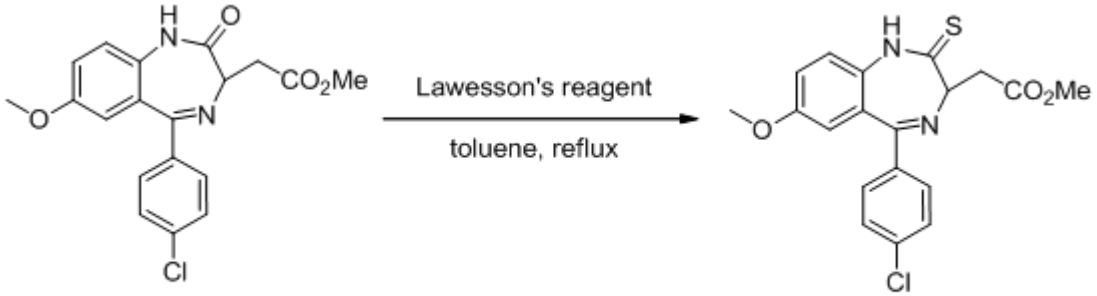

5 6

Methyl [5-(4-chlorophenyl)-7-(methyloxy)-2-thioxo-2,3-dihydro-1*H*-1,4-benzodiazepin-3-yl]acetate (6)

Lawesson's reagent (7.42 g, 18 mmol, 0.6 equiv.) was added to a solution of amide **5** (11.4 g, 30 mmol) in toluene (200 mL). The resulting mixture was stirred at reflux for 4 hours before being cooled and concentrated to dryness. The solid was taken up in DCM and the remaining solid was filtered and dried to afford thioamide **6** (9.5 g, 81% yield) as a pale yellow solid. ^{1}H NMR (300 MHz, $CDCl_3$) *d* 10.11 (br s, 1H), 7.48 (m, 2H), 7.34 (m, 2H), 7.18 (d, *J* = 8.9 Hz, 2H), 7.11 (dd, *J* = 8.9 and 2.8 Hz, 1H), 6.78 (d, *J* = 2.8 Hz, 1H), 4.39 (dd, *J* = 7.0 and 6.8 Hz, 1H), 3.76 (s, 3H), 3.75 (s, 3H), 3.66 (dd, *J* = 16.8 and 6.8 Hz, 1H), 3.38 (dd, *J* = 16.8 and 7.0 Hz, 1H). ^{13}C NMR (75 MHz, DMSO-d6) *d* 198.6, 171.3, 166.2, 155.4, 136.7, 135.4, 133.2, 131.1, 128.5, 128.4, 123.4, 119.0, 113.6, 63.8, 55.6, 51.3, 39.0. HRMS $(M+H)^+$ calculated for $C_{19}H_{18}{}^{35}ClN_2O_3S$ 389.0727; found 389.0714.

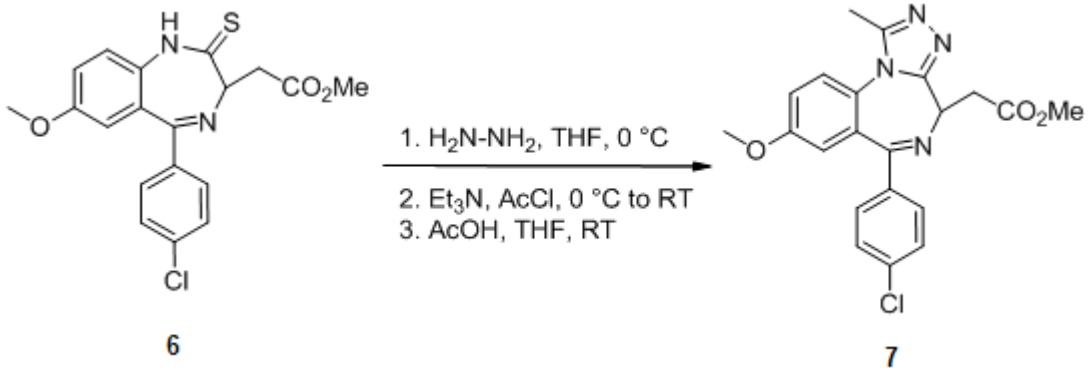

6 7

Methyl [6-(4-chlorophenyl)-1-methyl-8-(methyloxy)-4*H*-[1,2,4]triazolo[4,3-*a*][1,4]benzodiazepin-4-yl]acetate (7)

Hydrazine monohydrate (3.4 mL, 69.6 mmol, 3 equiv.) was added dropwise to a suspension of thioamide **6** (9.0 g, 23.2 mmol) in THF (300 mL) at 0°C. The reaction mixture was stirred for 5 hours at 0 °C. Et_3N (9.7 mL, 69.6 mmol, 3 equiv.) was then added slowly and AcCl (7.95 mL, 69.6 mmol, 3 equiv.) was added dropwise. The mixture was allowed to warm to room temperature for 16 hours before being concentrated under reduced pressure. The crude product was dissolved in DCM and washed with water. The organic layer was dried over Na_2SO_4, filtered and concentrated *in vacuo* to give the intermediate acetylhydrazone that was used without further purification R_f = 0.49 (DCM/MeOH:90/10). The crude acetylhydrazone (assumed 9.7 g) was suspended in THF (100 ml) and AcOH (60 mL) was added at room temperature. The reaction mixture was stirred at this temperature for 2 days before being concentrated under reduced pressure. The crude solid was triturated in *i*-Pr_2O and filtered to give the title compound **7** (8.7 g, 91% over 3 steps) as an off-white solid. ^{1}H NMR (300 MHz, $CDCl_3$) *d* 7.54-7.47 (m, 2H), 7.40 (d, *J* = 8.8 Hz, 1H), 7.37-7.31 (m, 2H), 7.22 (dd, *J* = 2.8 and 8.8 Hz, 1H), 6.89 (d, *J* = 2.8 Hz, 1H), 4.61 (dd, *J* = 6.4 and 7.8 Hz, 1H), 3.82 (s, 3H), 3.78 (s, 3H), 3.66 (dd, *J* = 7.8 and 16.9 Hz, 1H), 3.60 (dd, *J* = 6.4 and 16.9 Hz, 1H), 2.62 (s, 3H). ^{13}C NMR (75 MHz, DMSO-d6) *d* 171.1, 166.9, 157.4, 155.3, 150.9, 137.1, 135.5, 131.1, 129.2, 128.3, 126.3, 125.6, 117.8, 115.3, 55.8, 52.8, 51.6, 36.2, 11.5. HRMS $(M+H)^+$ calculated for $C_{21}H_{20}{}^{35}ClN_4O_3$ 411.1229; found 411.1245.

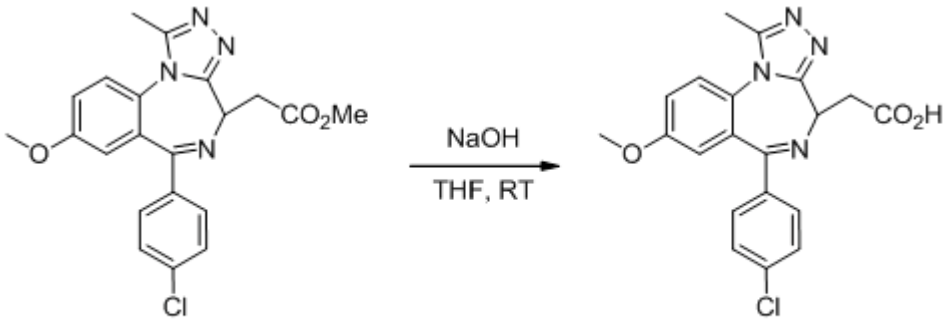

7 8

[6-(4-Chlorophenyl)-1-methyl-8-(methyloxy)-4*H*-[1,2,4]triazolo[4,3-*a*][1,4]benzodiazepin-4-yl]acetic acid (8)

1N NaOH (36.2 mL, 36.2 mmol, 2 equiv.) was added to a solution of ester **7** (7.4 g, 18.1 mmol) in THF (130 mL) at room temperature. The reaction mixture was stirred at this temperature for 5 hours before being quenched with 1N HCl (36.2 mL) and concentrated *in vacuo*. Water was then added and the aqueous layer was extracted with DCM (3 x) and the combined organic layers were dried over Na_2SO_4, filtered and concentrated

under reduced pressure to give the title compound **6** (7 g, 98% yield) as a pale yellow solid. ^{1}H NMR (300 MHz, $CDCl_3$) *d* 7.55-7.48 (m, 2H), 7.41 (d, *J* = 8.9 Hz, 1H), 7.38-7.31 (m, 2H), 7.22 (dd, *J* = 2.9 and 8.9 Hz, 1H), 6.90 (d, *J* = 2.9 Hz, 1H), 4.59 (dd, *J* = 6.9 and 6.9 Hz, 1H), 3.81 (s, 3H), 3.70 (dd, *J* = 6.9 and 25.7 Hz, 1H), 3.61 (dd, *J* = 6.9 and 25.7 Hz, 1H), 2.63 (s, 3H). ^{13}C NMR (75 MHz, DMSO-d6) *d* 172.1, 165.6, 157.4, 155.5, 150.8, 137.2, 135.4, 131.1, 129.2, 128.3, 126.3, 125.6, 117.9, 115.2, 55.8, 52.9, 36.5, 11.5. HRMS $(M+H)^+$ calculated for $C_{20}H_{18}{}^{35}ClN_4O_3$ 397.1067; found 397.1063.

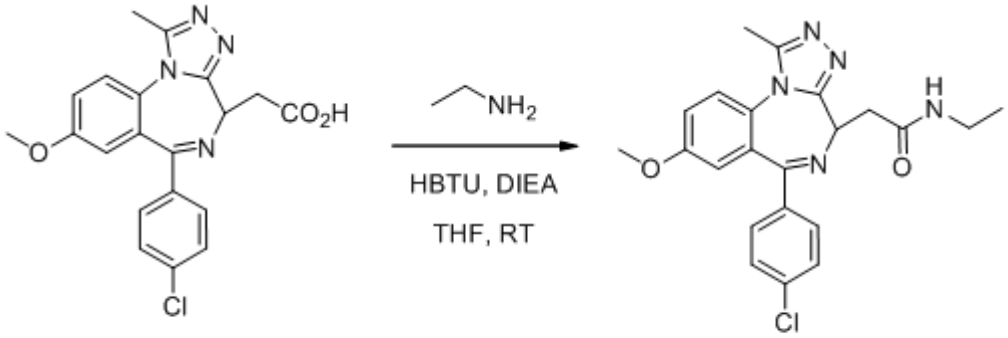

8 9

2-[6-(4-Chlorophenyl)-1-methyl-8-(methyloxy)-4*H*-[1,2,4]triazolo[4,3-*a*][1,4]benzodiazepin-4-yl]-*N*-ethylacetamide (9)

Diisopropylethylamine DIEA (4 mL, 22.7 mmol, 2 equiv.), followed by HBTU (8.6 g, 22.7 mmol, 2 equiv.) were added to a solution of acid **8** (4.5 g, 11.4 mmol) in THF at room temperature. The reaction mixture was stirred for 3 hours at this temperature and ethylamine (11.3 mL, 2M in THF, 22.7 mmol, 2 equiv.) was added dropwise. The mixture was stirred overnight before being concentrated under reduced pressure. The crude material was dissolved in DCM and washed successively with water, 1N NaOH and 1N HCl. The organic layer was dried over Na_2SO_4, filtered and concentrated *in vacuo*. The crude solid was recrystallised in CH_3CN to give the title compound **9** (4.1 g, 85% yield) as a white solid. R_f = 0.48 (DCM/MeOH:90/10). Mp 140-145 °C (becomes gummy). ^{1}H RMN (300 MHz, $CDCl_3$) *d* 7.53-7.47 (m, 2H), 7.39 (d, *J* = 8.9 Hz, 1H), 7.37-7.31 (m, 2H), 7.20 (dd, *J* = 2.9 and 8.9 Hz, 1H), 6.86 (d, *J* = 2.9 Hz, 1H), 6.40 (m, 1H), 4.62 (m, 1H), 3.80 (s, 3H), 3.51 (dd, *J* = 7.3 and 14.1 Hz, 1H), 3.46-3.21 (m, 3H), 2.62 (s, 3H), 1.19 (t, *J* = 7.3 Hz, 3H). ^{13}C NMR (75 MHz, DMSO-d6) *d* 169.2, 165.5, 157.4, 155.8, 150.7, 137.3, 135.4, 131.0, 129.3, 128.2, 126.4, 125.6, 117.8, 115.1, 55.8, 53.3, 37.6, 33.4, 14.8, 11.5. HRMS $(M+H)^+$ calculated for $C_{22}H_{23}{}^{35}ClN_5O_2$ 424.1540; found 424.1525.

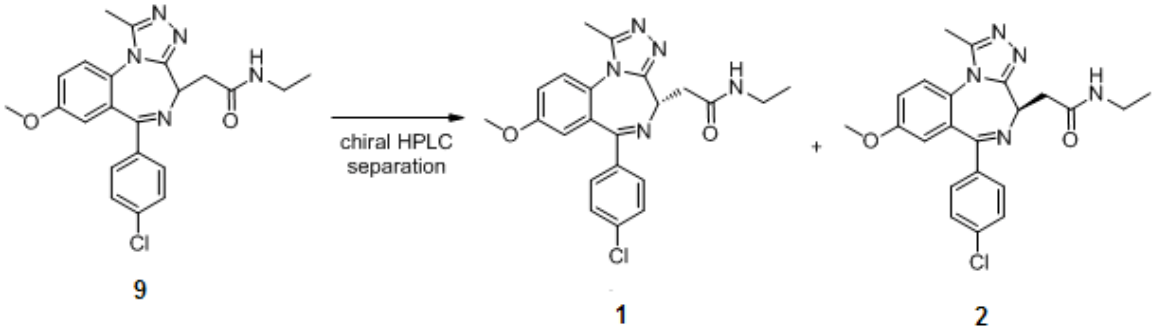

2-[(4*S*)-6-(4-chlorophenyl)-1-methyl-8-(methyloxy)-4H-[1,2,4]triazolo[4,3-a][1,4]benzodiazepin-4-yl]-*N*-ethylacetamide Cmpd 1 and **2-[(4*R*)-6-(4-chlorophenyl)-1-methyl-8-(methyloxy)-4H-[1,2,4]triazolo[4,3-a][1,4]benzodiazepin-4-yl]-*N*-ethylacetamide Cmpd 2**

Racemic mixture of 2-[(4-chlorophenyl)-1-methyl-8-(methyloxy)-4H-[1,2,4]triazolo[4,3-a][1,4]benzodiazepin-4-yl]-*N*-ethylacetamide **9** (200 mg) was separated by HPLC using a ChiralPack AD (250 x 20 mm id, 10 µm) column eluting with EtOH/hexane (60/40) as the mobile phase (Flow rate : 17 mL/min). **Cmpd 2** eluted at 5.21 min as the first peak. $[a]_D^{20}$ = + 88.1 (c = 1.0015 / MeOH). **Cmpd 3** came off at 24.28 min. $[a]_D^{20}$ = -87.7 (*c* 1.0015 / MeOH)[5]

Crystal structure of the BRD4-I-BET complex. *E.coli* expressed de-His-tagged Brd4-BD1(44-168) was crystallised in 1µL + 1µL hanging drops @ 4°C using Nextal plates over 20% PEG3350, 0.1M Na_2NO_3, 10% ethylene glycol. The protein was at 11.1mg/ml in 10mM HEPES pH7.5, 100mM NaCl and purified to homogeneity using a HisTrap column followed by gel fitration, Tev protease cleavage and gel filtration using a Sephadex 75 column. The I-BET compound was soaked into apo crystals for 4 days at 2mM. Soaked crystals were briefly transferred into 25% PEG3350, 0.1M Na_2NO_3, 15% ethylene before flash freezing into liquid nitrogen. Data from a single crystal was collected at the ESRF (European Synchrotron Radiation Facility, Grenoble), processed to 1.60 Å using mosflm and scaled using scala (CCP4). Molecular replacement solution was performed with 2oss.pdb using Phaser (CCP4). The $P2_12_12_1$ cell (a=b=g=90˚, a=37.428Å b=44.333Å, c=78.345Å) has a single molecule in the ASU. Model building was performed using Coot [6] and refined using refmac (Collaborative Computational, 1994). The I-BET compound could easily be modelled into the difference density. The statistics for the data collection and refined coordinates are given in (Supplementary Fig

2a). All structure data has been deposited in the RCSB Protein Data Bank RCSB with PDB ID code 3P5O.

Isothermal titration calorimetry. ITC titrations were carried out using a Microcal VP-ITC in 20mM Hepes, pH 7.5, 100mM NaCl at the temperatures indicated in Supplementary Fig 1d. Compound concentrations were determined by NMR and protein concentrations by A280 measurements. Typically 10-20 μM of compound was placed in the cell and 50-100 μM protein was titrated into this at 25°C to achieve at least a final excess of 0.8:1 for his-tagged tandem bromodomain constructs. Injections were performed using protein in the syringe rather than compound due to avoid any potential limitations in compound solubility. The data was fitted with Origin (Microcal version).

Fluorescence resonance energy transfer (FRET) titrations. I-BET was titrated against BRD2 (200nM), BRD3 (100nM) and BRD4 (50nM) in 50mM HEPES pH7.5, 50mM NaCl, 0.5mM CHAPS in the presence of tetra-acetylated Histone H4 peptide (200nM) (Millipore, cat 12-379). After equilibrating for 1 hour, the bromodomain protein : peptide interaction was detected using FRET following the addition of 2nM Europium cryptate labelled streptavidin (Cisbio610SAKLA) and 10nM XL-665-labelled anti-6His antibody (Cisbio 61HisXLA) in assay buffer containing 0.05% (v/v) BSA and 400mM KF. Plates were read using an Envision Plate reader (excitation 320nm, emission 615 nm and 665nm).

Reagents and Cell Stimulations

LPS (*Escherichia coli* 0111:B4, 100 ng/mL) was purchased from Sigma. TNF (50 ng/mL) was purchased from eBioscience. Bone marrow-derived macrophages (BMDMs) were differentiated from bone marrow extracted from the femur and tibia of 6-8 week female C57BL/6 mice using 5 ng/mL each of recombinant M-CSF and IL-3 (Peprotech) for 7 days as described. BMDMs were pre-incubated with 1 μM of I-BET dissolved in dimethyl sulfoxide (DMSO) or a DMSO vehicle control for 30 minutes prior to stimulation.

Gene expression analysis by microarray

BMDMs were stimulated with LPS (100 ng/mL) for indicated time periods. 500 ng of total RNA from 3 independent samples per group were used to prepare biotin-labeled RNA using Ambion Illumina TotalPrep RNA Amplification Kit (Applied Biosystems) and

hybridized to Illumina MouseRef-8 v2.0 expression BeadChip kits. The chips were scanned using Illumina BeadArray Reader following by analysis using the R/Bioconductor BioC 2.5 suite of tools (www.bioconductor.org/). The quality of raw expression data was assessed by standard approaches and subjected to background adjustment and quantile normalization using "beadarray"[7]. Log_2 scaled data was used for linear modelling, differential expression profiling and relevant graphical representations using the LIMMA library[8]. Associated transcript annotation was retrieved from the illuminaMousev2BeadID library. The microarray data sets are available in the Gene Expression Omnibus (GEO) under the accession number GSE21764.

RNAi-mediated knockdown of Brd2, Brd3 and Brd4 in bone marrow-derived macrophages

$2x10^5$ macrophages were seeded overnight in a 24-well plate and transfected with siRNA oligonucleotides targeted to mouse *brd2, brd3*, *brd4* or a scrambled control (5 nM, Thermo Scientific Dharmacon 'siGENOME SMARTpool') using HiPerfect Reagent (QIAGEN) and used at 48 hours. Mock-transfected cells were given HiPerfect Reagent only. Cells were stimulated as described in Reagents and Cell Stimulations and gene expression was assessed by qPCR.

Quantitative PCR

BMDMs were treated with DMSO, 1 μM I-BET or 1 μM of an inactive enantiomer of I-BET, GSK525768 (inactive I-BET) for 30 minutes before the addition of LPS for indicated times, and the total RNA was extracted using an RNase minikit (Qiagen) according to the manufacturer's protocol. RNA was DNase treated using an RNase free DNase set (Qiagen) and cDNA was synthesized using reagents supplied with a first strand cDNA synthesis kit (Roche). Quantitative real-time PCR was performed using SYBR Green (Roche) on a Roche Lightcycler 480. Primer sequences are available upon request.

Chromatin immunoprecipitation (ChIP) and ChIP sequencing

For ChIP experiments, BMDMs were stimulated as described above and ChIP was performed as described previously [9, 10]. To cross-link proteins to the DNA, cells were treated with 1% formaldehyde for 10 minutes and the cross-linking reaction was

terminated by addition of glycine to a final concentration of 0.125 M. Cross-linked chromatin was sonicated using a Biorupter (Diagenode) to generate DNA-fragments of approximately 200 to 600 bp in length. Antibodies to precipitate the chromatin fragments were pre-bound to Invitrogen Dynal magnetic beads (Invitrogen Dynabeads anti-mouse M-280 or Dynabeads anti-rabbit M-280) in 0.5% BSA/PBS. The following antibodies have been used: H3 (Abcam, ab1791), H3K4me3 (Millipore, 17-614), H4Ac (Millipore, 06-866), H4K5Ac (Millipore 07-327), H4K8Ac (Millipore 07-328), H4K12Ac (Millipore 07-595), H3Ac (Millipore 06-599), BRD2 (Bethyl Laboratories A302-583A), BRD3 (Bethyl Laboratories A302-368A) BRD4 (Bethyl Laboratories A301-985A or Abcam ab84776), CDK9 (P-TEFb; Santa Cruz, sc-8338), Pol II (Abcam, ab5408) and Pol II S2 (Abcam, ab5095). ChIP assays were performed using $1x10^6$ cells (for Pol II and Pol II S2), $2x10^6$ cells (for BRD3 and BRD4) or $3x10^6$ (for BRD2 and P-TEFb (CDK9) and 2 μg of antibody coupled to 20 μL beads. ChIP-Seq was performed using $1x10^7$ cells and 7 μg antibody coupled to 70 μL magnetic beads (for H3, H3K4me3, Pol II, Pol II S2, BRD2 and BRD3) or $2x10^7$ cells and 14 μg antibody coupled to 140 μL beads (for H4Ac, H4K5/K8/K12Ac, H3Ac, BRD4 and P-TEFb (CDK9)). Beads were added to the cell lysates. After overnight incubation, beads were washed 8x in modified RIPA wash buffer (50 mM HEPES [pH 7.6], 100 mM LiCl [for H3Ac, H4Ac, H4K5/K8/K12Ac, BRD2/3/4 and P-TEFb (CDK9)] or 300 mM LiCl [H3, H3K4me3, Pol II and Pol II S2], 1mM EDTA, 1% NP-40 and 0.7% Na-deoxycholate) and 1x in TE containing 50 mM NaCl. Elution of DNA was performed in TE buffer containing 1% SDS. After overnight cross-link reversal at 65^0C, RNase digestion and Proteinase K digestion, ChIP DNA and input DNA were purified using the QIAGEN Quiaquick PCR purification kit. For regular ChIP and for validation of ChIP-Seq, ChIP DNA was analyzed via qPCR using SYBR Green (Roche) and the Lightcycler 480 (Roche). Primer sequences are as follows: il6-f: tgtgggattttcccatgagt; il6-r: tgccttcacttacttgcagaga; tnf-f: ggactagccaggagggagaa; tnf-r: tgtcttttctggagggagatgt; Il1b-f acttgcacaaggaagcttgg; il1b-r ccaagggaaaatttcacagc; nfkbia-f ccacttacgagtctccgtcct; nfkbia-r aggagtacgagcaaatggtga.

For ChIP-Seq, 30 μL of ChIP DNA was used to generate blunt-ended DNA using reagents supplied with the Epicenter DNA ENDRepair kit (Epicenter Biotechnologies). The end-repaired DNA was purified using the QIAGEN Quiaquick PCR purification kit. Using Klenow Fragment (NEB) “A” bases were added to the DNA. DNA was purified using the QIAGEN MinElute kit. T4 DNA ligase (NEB) was used for ligation of Illumina/Solexa adapters to the DNA fragments. The adaptor-ligated DNA was purified

with the QIAGEN MinElute kit. The DNA fragments were subjected to 18 cycles of PCR using the Illumina/Solexa primers 1.0 and 2.0 to generate the ChIP-Seq libraries. The ChIP-Seq libraries were then purified with the QIAGEN MinElute kit. Samples were sequenced on the Illumina GAIIx platform for 36 cycles, and raw sequencing data were processed using the onboard SCS/RTA software version 2.6 yielding 36bp reads. Sequencing kits used were version 4 sequencing kits. Sequencing reads were aligned to the mouse genome (NCBI37/mm9) using Bowtie[11]. Reads were kept if they aligned with 2 errors or less and did not align to more than one location in the genome. Sequencing reads were extended 100bp in the 3' direction, and the number of reads per 100bp bin was calculated. Visualization of the integrated enrichment values for each ChIP sample was obtained by calculating the average enrichment value for specific sets of genes in 100bp increments upstream and downstream of the TSS for the distance indicated. Aspects of this analysis utilized the CEAS package[12]. Browser tracks were displayed using the Integrative Genome Viewer, and made using the IGVtools count function set for 100bp extensions in the 3' direction and 25bp windows. Values are reported as reads per million mapped reads, utilizing version 1.5.2 of the browser. The ChIP-seq data sets are available in the Gene Expression Omnibus, accession number GSE21910.

Histone Acetyl Transferase IC_{50} profiling. The effect of I-BET on the catalytic activity of pCAF, GCN5, p300 and CBP was determined in a HotSpot HAT activity assay by Reaction Biology Corporation according to the company's standard operating procedure. In brief, the recombinant catalytic domains of pCAF (aa 492-658), GCN5 (aa 497-663), p300 (aa 1284-1672) or CBP (aa 1319-1710) were incubated with histone H3 as substrate and [Acetyl-3H]-Acetyl Coenzyme A as an acetyl donor in reaction buffer (50 mM Tris-HCl (pH 8.0), 50 mM NaCl, 0.1 mM EDTA, 1 mM DTT, 1 mM PMSF, 1% DMSO) for 1 hour at 30^{o}C in the presence or absence of a dose titration of I-BET. Histone H3 acetylation was assessed by liquid scintillation. Anacardic acid or curcumin served as controls that inhibit pCAF, GCN5 and CBP or p300 activity, respectively. Data was analyzed using Excel and GraphPad Prism software for IC_{50} curve fits.

Classification of primary and secondary response genes by kinetic analysis.
We wrote an algorithm in R (http://www.r-project.org/) to classify genes as either Primary Response Genes ('PRGs') or Secondary Response Genes ('SRGs') based on their microarray-measured expression kinetics in LPS-stimulated macrophages (accession

number GSE21764). Briefly, PRGs were required to reach a maximum expression at 1 hour and diminish at 2 hours (0<1h>2h) whilst SRG had to rise later at 2 or 4 hours (0h=1h (<1.5 fold difference), 2h>1h, 4h≥2h). Based on published PRG and SRG genes [13-15], we classified known PRGs and SRGs correctly 67% (n=45) and 69% (n=29) of the time, respectively.

I-BET pharmacokinetics. Balb/c mice were injected with I-BET via the tail vein at a dose of 30mg/kg. Blood samples from all mice were obtained via a separate tail vein at the times indicated. The concentrations of I-BET in the blood were determined after acetonitrile protein precipitation by reverse phase HPLC using an Ascentis Express C18 column and detected using a specific MS/MS method employing a heat assisted electrospray interface in positive ion mode (PE SCIEX API 4000). Standard curves and quality control samples for the determination of I-BET were prepared on the day of the assay. The lower limit of quantification for I-BET was 0.002 μM. The assay was linear for I-BET up to 47.2 μM. Pharmacokinetic data analysis was undertaken using WinNonlin v4.1a software.

***In vivo* models.**

LPS-induced endotoxic shock. 6-week old female C57BL/6 mice were obtained from Charles River Laboratories and were housed under specific pathogen free conditions under the regulations of The Rockefeller University animal facility. A pre-determined lethal dose (5 mg/kg) of LPS was injected intraperitoneally and survival was monitored. I-BET (30 mg/kg, dissolved in 20% beta-cyclodextrin, 2% DMSO in 0.9% saline) or a solvent control was given intravenously (retro-orbital injection) 1 hour before or 1.5 hours after LPS administration. Cytokine concentrations in mouse serum 2 hours after LPS injection were determined using a Mouse proinflammatory 7-Plex Assay (IL1b, IL12p70, IFNg, IL-6, KC/GRO, IL-10, TNF) multi-spot ELISA assay (Meso Scale Discovery) according to the manufactures protocol.

Salmonella-induced endotoxic shock. Salmonella typhimurium strain IR715, which was transformed with the GFP expressing plasmid pSMC21 by electroporation was a gift from Markus Grammel at The Rockefeller University. A pre-determined lethal dose of $5x10^9$/kg heat-killed (5 minutes at 94^oC) *Salmonella typhimurium* was administered intravenously (retro-orbital injection) and mortality was monitored. I-BET (30 mg/kg,

dissolved in 20% beta-cyclodextrin, 2% DMSO in 0.9% saline) or a solvent control was given intravenously 1 hour before.

Cecal Ligation Puncture (CLP) was performed as described[16]. Briefly, 10-12-week old female mice (n=8 per group) were aneasthetized with Tribromoethanol (Avertin®) at a minimal dose (30 mg/kg in 37°C PBS, intraperitoneal injection). During anaesthesia and operation mice were kept at 37°C. An abdominal midline incision was then performed and the cecum was isolated. The cecum was ligated 5 mm from the cecal tip, away from the ileocecal valve, the ligated cecal stump was lifted gently by blunt forceps and perforated by two "through and through" punctures (22-gauge needle) outside of the blood vessels area. The cecum was allowed to retrieve back into the peritoneal cavity with minimal external intervention and the abdomen was sealed. During operation and recovery from anesthesia mice were immobilized on the back. After recovery, mice were kept at 37°C and their mobility was limited by extra bedding. I-BET, dissolved in solvent, sonicated and filtered, was administered intravenously into a tail vein (30 mg/kg) at a slow rate and only after recovery of mice from anaesthesia (as administered immediately after surgery had a negative impact on recovery from anaesthesia) and then every 12 hours post surgery.

1. Jang, M. K. et al. The bromodomain protein Brd4 is a positive regulatory component of P-TEFb and stimulates RNA polymerase II-dependent transcription. Mol Cell 19, 523-34 (2005).
2. Yang, Z. et al. Recruitment of P-TEFb for stimulation of transcriptional elongation by the bromodomain protein Brd4. Mol Cell 19, 535-45 (2005).
3. Denis, G. V. et al. Identification of transcription complexes that contain the double bromodomain protein Brd2 and chromatin remodeling machines. J Proteome Res 5, 502-11 (2006).
4. Stafford, J. A. et al. Identification and structure-activity studies of novel ultrashort-acting benzodiazepine receptor agonists. Bioorg Med Chem Lett 12, 3215-8 (2002).
5. Walsh, D. A. et al. Antiinflammatory agents. 3. Synthesis and pharmacological evaluation of 2-amino-3-benzoylphenylacetic acid and analogues. J Med Chem 27, 1379-88 (1984).
6. Emsley, P. & Cowtan, K. Coot: model-building tools for molecular graphics. Acta Crystallogr D Biol Crystallogr 60, 2126-32 (2004).
7. Dunning, M. J., Smith, M. L., Ritchie, M. E. & Tavare, S. beadarray: R classes and methods for Illumina bead-based data. Bioinformatics 23, 2183-4 (2007).

8. Smyth, G. K. Linear models and empirical bayes methods for assessing differential expression in microarray experiments. Stat Appl Genet Mol Biol 3, Article3 (2004).
9. Lee, T. I., Johnstone, S. E. & Young, R. A. Chromatin immunoprecipitation and microarray-based analysis of protein location. Nat Protoc 1, 729-48 (2006).
10. Goldberg, A. D. et al. Distinct factors control histone variant H3.3 localization at specific genomic regions. Cell 140, 678-91.
11. Langmead, B., Trapnell, C., Pop, M. & Salzberg, S. L. Ultrafast and memory-efficient alignment of short DNA sequences to the human genome. Genome Biol 10, R25 (2009).
12. Shin, H., Liu, T., Manrai, A. K. & Liu, X. S. CEAS: cis-regulatory element annotation system. Bioinformatics 25, 2605-6 (2009).
13. Hargreaves, D. C., Horng, T. & Medzhitov, R. Control of inducible gene expression by signal-dependent transcriptional elongation. Cell 138, 129-45 (2009).
14. Ramirez-Carrozzi, V. R. et al. A unifying model for the selective regulation of inducible transcription by CpG islands and nucleosome remodeling. Cell 138, 114-28 (2009).
15. Ramirez-Carrozzi, V. R. et al. Selective and antagonistic functions of SWI/SNF and Mi-2beta nucleosome remodeling complexes during an inflammatory response. Genes Dev 20, 282-96 (2006).
16. Rittirsch, D., Huber-Lang, M. S., Flierl, M. A. & Ward, P. A. Immunodesign of experimental sepsis by cecal ligation and puncture. Nat Protoc 4, 31-6 (2009).